UNITED STATES
DEPARTMENT OF THE INTERIOR
BUREAU OF MINES
Pittsburgh, Pennsylvania

HYPERGOLIC IGNITION AND COMBUSTION PHENOMENA
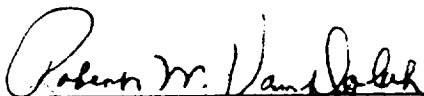# IN THE PROPELLANT SYSTEM AEROZINE-50/N_2O_4

FINAL REPORT

April 1, 1965 to March 31, 1967

by

Henry E. Perlee
Yael Miron
Harry James
Theodore Christos

APPROVED:

Robert W. Van Dolah
Research Director, Explosives Research Center
Bureau of Mines
4800 Forbes Avenue
Pittsburgh, Pennsylvania 15213

for

Manned Spacecraft Center
National Aeronautics & Space Administration
Houston, Texas

I. INTRODUCTION

This is the final report of a three-year effort conducted at the Explosives Research Center of the Bureau of Mines concerned with adverse hypergolic ignition phenomena.

Recent simulated high-altitude start test firings of 100-lb thrust pulse modulated Apollo RCS engines using the propellant combination Aerozine-50/nitrogen tetroxide have resulted in explosive ignitions (hard starts) that permanently damage the engine complex. Although to date such incidents have been limited to low thrust attitude control engines, there is no evidence that larger engines are not susceptible to similar phenomena.

These engine failures during simulated altitude starts have prompted the Manned Spacecraft Center (MSC), Houston, Texas, to investigate their occurrence, and at the request of MSC, the Explosives Research Center of the Bureau of Mines has undertaken this problem. This effort consisted of two programs, a literature and industry survey and an experimental study designed to supplement the information disclosed in the survey. The results of both these programs, as related directly to the hard start problem, are included in this report.

The survey section of this report covers all the work, including that reported by the Bureau to date, concerned with the various pressure spiking processes believed to occur in the engines during the initial period of engine start. These include manifold spiking, heterogeneous combustion and condensed phase combustion. Manifold spiking is evidenced by a rapid sequence of strong pressure spikes in the engine's nitrogen tetroxide feed lines following valve opening. Heterogeneous combustion concerns the ignition and initial propagation of flame through the propellant spray-vapor system accumulated in the engine combustion chamber during the pre-ignition period. Finally, condensed phase combustion is the burning of solid or liquid materials (reactants and/or product material formed during the preignition or post combustion periods) that have accumulated on the engine's interior chamber walls. The study concerning the condensed phase materials has to date been the primary interest of the Explosives Research Center; experimental details and observations of this investigation are described in a later section of this report to avoid confusing experimental details with information contained in the survey.

The Bureau's experimental effort involved: (1) the combustion characteristics of the propellants individually and jointly, (2) the identification of preignition reaction products, and (3) the physical and combustion characteristics of these products in relation to their presence in these engines. The structural and inertial responses of small rocket engines to internal explosions were also studied. Propellants used in these studies consisted of the common hydrazine fuels: hydrazine (N_2H_4), monomethylhydrazine (MMH),

unsymmetrical dimethylhydrazine (UDMH),and Aerozine-50 (A-50, a 50:50 mixture by weight of N_2H_4 and UDMH). The oxidant was nitrogen tetroxide N_2O_4.

A section describing some principles of combustion has been included to familiarize the reader with the concepts and terms necessary to understand this report. Those readers already well versed in basic combustion principles can omit this section without any loss of continuity.

II. COMBUSTION PRINCIPLES

Combustion involving gases or condensed-phase material can be either deflagrative or detonative. Deflagrative combustion is characterized by the subsonic propagation of the combustion zone relative to the burning material. Detonative combustion is characterized by supersonic propagation of the combustion front relative to the unburned material. With subsonic propagation of a deflagration in a gas mixture, the pressures developed in the combustion zone are readily dissipated into the environment. Consequently, deflagrations are characterized by a small pressure differential across the combustion zone, that is, the ratio of the pressures across the front is approximately one. Specifically, if the propagation velocity of the combustion zone is less than about 1/10 the speed of sound relative to the unburned material, the pressure ratio is almost one. Thus, when a gas mixture in a closed volume burns deflagratively, the increase in pressure due to combustion is uniformly distributed (hydrostatically) throughout the mixture; as the propatation velocity increases, approaching the speed of sound, the pressure ratio rises rapidly.

A detonation, on the other hand, exhibits large pressure ratios across the flame front, typically 20 to 50 for gas mixtures. For example, consider the cylindrical closed vessel 12 inches long and several inches in diameter, shown in figure 1E, containing a fictitious gas mixture at a pressure of 1 atmosphere, capable of supporting both deflagrative and detonative combustion processes depending on the type of ignition. Assume that (1) the mass flux through the flame front is constant and independent of the pressure, (2) the gas pressurization processes occur adiabatically, (3) the pressure ratio across the deflagration is 1 and across the detonation, 13, and (4) the corresponding burning velocities (speed of flame relative to unburned gas immediately ahead of the flame) are 10 and 10,000 feet per second, respectively. Figure 1C shows three positions of the flame front as it traverses the vessel 4, 8, and 12 inches from the ignition source (I). Figures 1A and 1D show the spatial pressure distributions in the vessel corresponding to the three flame front positions for the deflagration and detonation.

In deflagrative combustion, a volume of gas expands as it traverses the flame front as a result of thermal and molecular changes, forcing the flame to a speed greater than its normal burning velocity. Usually this
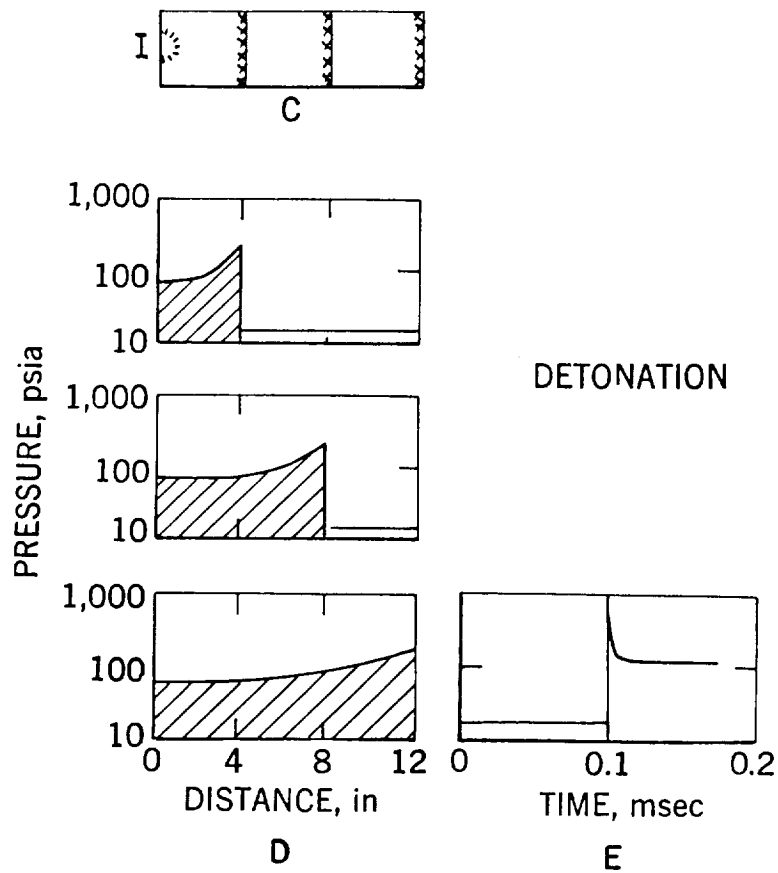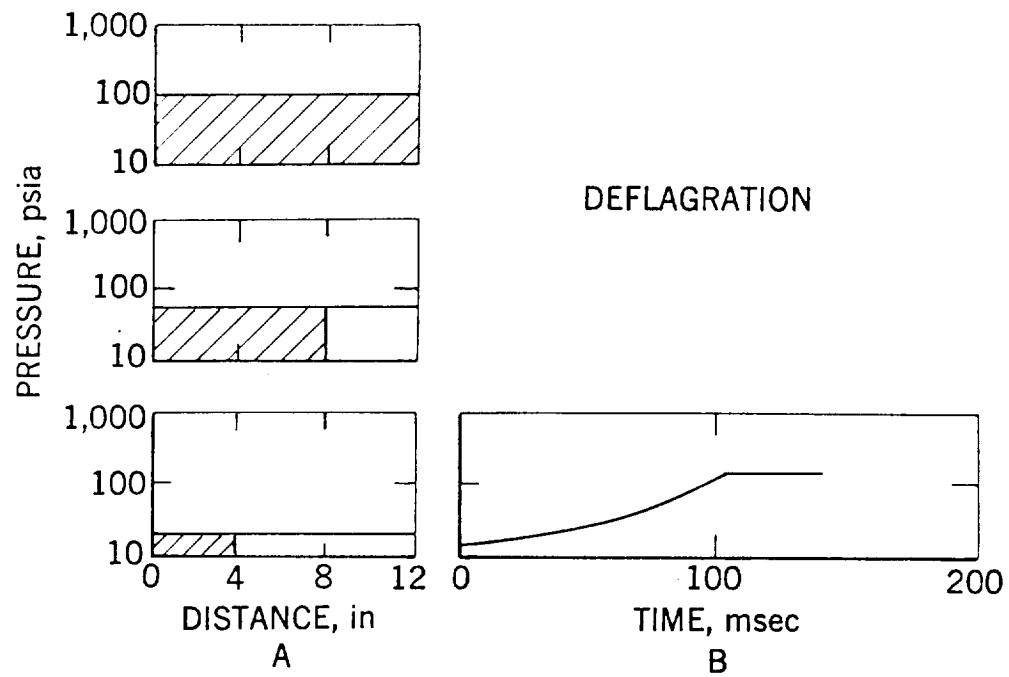
Figure 1: Pressure histories for deflagrative and detonative combustion.

PX3-103
549

increase amounts to a factor of about 10 initially, decreasing to 1 at
the end of the combustion process. Thus, initially the flame front propa-
gates away from the ignition source with a speed of 10 x 10 or 100 feet
per second relative to the vessel. Since its speed relative to the unbruned
gas is 10 feet per second, which is 1 percent the speed of sound (1,000 feet
per second) in the unburned mixture, the pressure waves developed by the
flame front are rapidly dissipated in the surrounding mixture, resulting
in a uniform pressure distribution throughout the mixture. This is illus-
trated in figure 1C where the pressure of the mixture (burned and unburned)
increases uniformly as the flame propagates down the tube, attaining a
final value of 100 psia when combustion is complete.

On the other hand, in detonation, the flame speed is supersonic relative
to the unburned gas (10,000 feet per second, compared with a sound speed of
1,000 feet per second) and there can be no acoustical transmission of energy
ahead of the combustion front. Consequently, an abrupt pressure discontinuity
or shock wave is formed followed immediately by the combustion zone. The
result is the large pressure spike shown in figure 1D, where the pressure
rises abruptly from an initial value of 15 psia in the unburned mixture to 15
x 13 or 200 psia, behind the shock front (typically, the detonation pressure
is twice the constant volume combustion pressure) and then falls sharply, but
continuously, to about 35 percent of the peak value or 70 psia.

Since it has been assumed in this discussion that the terminal (burned
and unburned) states of the constituents for the deflagration and detonation
processes are the same, the final burned gas pressure will be equal (100 psia).
It should be noted that for a detonation process, a pressure transducer
located in the end wall of the vessel, opposite the ignition source, fails
to detect any change in pressure until the detonation wave reaches it, whereas,
for a deflagration, a transducer similarly placed continuously follows the
uniform pressure increase during the entire combustion process (figure 1B and
1E). When a detonation wave normally impacts a rigid surface the applied
pressure is a combination of the detonation's intrinsic (hydrostatic) pressure
(figure 1D) and the pressure produced by reversal of the momentum of the
moving gases. This normally results in a pressure spike, applied to the wall
following reflection of the detonation, equal to about 2.5 times the intrinsic
pressure,[1]/ or about 500 psi in this example (figure 1E). Although the final
steady-state pressures for both processes are the same, a detonation delivers
a high impulse load to the vessel walls accounting for much of its destructive
nature. Furthermore, since the thickness of this high pressure zone increases
with distance of travel (figure 1D), its destructiveness increases correspond-
ingly with travel. Normally, if the necessary thermodynamic and chemical
kinetic data concerning the various reactants and products are available, it
is not difficult to calculate detonation pressures, temperatures, and velocities.
Unfortunately, in general, similar calculations are not available for deflagra-
tions, although it is possible to reliably estimate flame temperature and
product gas compositions.

A similar theory can also be applied to condensed-phase systems with the following additional considerations. As the speed of sound in condensed phase materials is normally about 5,000 feet per second, compared with 1,000 feet per second for gases, it is apparent that a subsonic combustion zone traveling in the condensed-phase material can be supersonic with respect to the surrounding gas. Consequently, although the combustion is deflagrative in the condensed phase, it produces a pressure field (blast wave) in the surrounding gas that behaves as though it were a gaseous detonation. Thus, usually it is not often possible to distinguish between condensed-phase detonations and deflagrations by studying the effects of combustion processes in the surrounding gas environment; these phenomena are usually termed detonation-like.

Blast waves produced in the environment of condensed-phase explosions have spatial pressure distributions similar to detonation waves except that the pressure decays less rapidly behind the shock front. Since the combustion zone is absent, its intensity (spike level) decreases more rapidly with distance of travel, usually decreasing as the reciprocal of the cube of the distance for spherical charges and the reciprocal of the square of the distance for cylindrical charges.

The following empirical relation for estimating vessel explosion design pressures as a function of vessel volume and weight of explosive has been developed by Loving:[2]

$$P = K \frac{W}{V} ,$$

where P is an equivalent hydrostatic pressure in psi, which may be used as the design pressure in standard calculations, W is the weight of explosive in pounds, V is the volume of the vessel in cubic feet, and K is a constant. This constant is different for each explosive ($K = 2 \times 10^4$ for TNT, 1.5×10^4 for PETN, and 7×10^3 for 40 percent dynamite); the actual value of the constant depends on the strength and completeness of reaction for the explosive decomposition. This relationship has been used for charge weights up to 5,000 grams.

Of the propellants of interest in this study, hydrazine has been most intensely investigated, probably because it is the only propellant included in this study that undergoes monopropellant combustion in the vapor phase.

A Bureau of Mines[3] study in 1949 showed that liquid hydrazine was not susceptible to detonation, although ballistic mortar experiments with the liquid gave a TNT equivalence of 135 percent when fired with an Army special detonator (J-2); this anomalous behavior will be discussed in a later section. Detonability experiments, in which liquid hydrazine (N_2H_4) in steel and plastic tubes (7.25 in. long and 0.875 in. id) was heated to 105°C and fired at one end with a (20-gram) tetryl charge, showed no more damage than a similar

water-filled tube fired under the same conditions. In a later Bureau of Mines' study[4]/neither liquid N_2H_4 at 90°C nor liquid UDMH at 53°C exhibited any tendency to detonate in an aluminum tube (3 in. long, 1.0 in. id) when fired at one end with 100 grams of tetryl.

Other investigators have studied the detonability of N_2H_4 vapors. In general, it has been found that a low energy ignition source, such as a weak electrical spark or hot wire, does not initiate detonation of N_2H_4 vapors in tubes up to 3 feet long and several inches in diameter. However, shocks generated by $H_2 + O_2$ or $C_2H_2 + O_2$ detonations consistently initiate detonation of N_2H_4 vapors.[5,6]/

III. IGNITION SPIKE SURVEY

Although it has not yet been determined whether the three pressure spiking processes described above (manifold, heterogeneous or condensed phase) are related, this possibility should not be overlooked. Until this has been determined, it must be assumed that a connection may exist. However, because of the time delay of about 3 milliseconds between the appearance of manifold spiking and ignition in these 100-lb thrust engines, it presently seems remote that they are related. In view of the uncertain interdependency of these three phenomena, our discussion must include them all.

Manifold Spiking: As previously noted, manifold spiking, or "Zot" as it has sometimes been called, is evidenced by a rapid sequence of pressure spikes in the N_2O_4 line within a few milliseconds following valve opening. Initially, this phenomenum was thought to be a water-hammer effect. However, its intensity and the absence of similar phenomenum in the fuel lines led investigators to seek other explanations.

One of the first alternate explanations was suggested by Minton and Zwick[7]/ who showed that, for the particular engine in question, the N_2O_4 manifold volume empties its liquid contents before the fuel manifold, permitting the fuel vapors in the combustion chamber to condense in the capillaries of the N_2O_4 manifold. This condensation process is assisted by the continual "breathing" of the empty N_2O_4 manifold as a result of chamber pressure oscillations during the post combustion period. Subsequent restart of the engine causes explosions in the N_2O_4 manifold when the entering N_2O_4 encounters the condensed fuel. These investigators attempted to demonstrate the feasibility of this hypothesis by artifically seeding the N_2O_4 manifold volume of a clean engine with liquid fuel prior to firing. Since the shape of the manifold pressure signature obtained in these experiments was similar to those obtained under normal low pressure operating conditions, the authors concluded that their hypothesis was correct. This explanation assumes that the N_2O_4 manifold empties completely, a very unlikely assumption considering the internal complexity of the manifold's geometry. It seems reasonable to believe, in view of recent studies, that the vapors of any liquid N_2O_4 remaining in the manifold

will react with the fuel deposited in the manifold capillaries producing hydrazine nitrate. These hydrazine nitrate deposits would in turn react with the entering liquid N_2O_4 on restart to produce the observed pressure spiking.

Another explanation for the manifold spikes has been advanced by researchers at Dynamic Science Corporation (DSC) who contend that the propagation of a shock wave through cavitated liquid N_2O_4 produces shock amplification by means of the exothermic reaction: $2NO_2 \rightarrow N_2O_4$. In exploratory studies in which boiling N_2O_4 was impacted with gas shocks having a pressure ratio of about 6, they measured pressure spikes in the boiling liquid having ratios as large as 200, corresponding to a pressure amplification of 30. These investigators believe that, following valve opening in an engine, the N_2O_4 in the feed line cavitates (boils), and upon reaching various restrictions in the manifold, a water-hammer effect is produced which is amplified by the above exothermic reaction in the cavitated system, thus producing the observed pressure spiking.

However, an alternate explanation might be presented to account for shock amplification in cavitated liquids, namely, the collapse of vapor cavities in a pressure gradient. An extensive survey of the dynamics of a collapsing bubble has been made by Ivany.[8] In particular, the experiments of Naude and Ellis,[9] Shutler and Mesle,[10] and Benjamin and Ellis[11] have established the existence of shocks and jets during the collapse of bubbles in pressure gradients. Recent experiments conducted at the Bureau with shocks and collapsing bubbles in liquids have demonstrated that hypervelocity jets[12] result from shock and bubble interaction. These jets in turn give rise to spherical shock waves in the bulk liquid, which by Huygen's principle, coalesce into a shock front adding to the existing or driving shock. The extent of shock amplification by such a process depends, among other things, on the size and number density of the contained bubbles and on the shock strength. Although a quantitative analysis of this shock--bubble interaction remains to be found, a qualitative explanation has been formulated in reference.[11]

It is apparent from this discussion that a satisfactory explanation of manifold pressure spiking is not available and further studies are required to determine the exact nature of the phenomenum.

Heterogeneous Combustion: Heterogeneous combustion concerns the burning of a mixture of gaseous and condensed-phase material such as is found in the liquid propellant rocket engine combustion chamber. In the case of the hypergolics this constitutes a system containing droplets and vapors of the two propellants and any gas or condensed-phase material formed as a result of chemical reaction during the preignition period or remaining from previous pulses.

Heterogeneous combustion has not been investigated to the same extent as homogeneous combustion; however, both systems exhibit deflagrative and detonative combustion phenomena. Heterogeneous deflagrations have been

studied for many years, but, as in the case of homogeneous systems, their complexity prevents many generalizations regarding their combustion characteristics; therefore it is usually necessary to study each system individually. Initially, there was some skepticism regarding the detonability of sprays due to the extended reaction zone arising from the anticipated leisurely droplet evaporation processes. However, it was found that droplet shatter behind shock fronts provides a very rapid process for converting drops to vapor. Williams[13] was one of the first investigators to examine the theoretical ramifications of heterogeneous detonations, and it was his suggestion that droplet shatter might provide the mechanism for sustaining heterogeneous detonation. Webber[14] and Cramer[15] conducted experiments on the combustion of diethylcyclohexane spray oxygen mixtures using a shock wave to ignite the mixture. They observed the propagation of a steep-fronted, high velocity wave which they termed "detonation-like". Busch, Laderman and Oppenheim[16] pursued a theoretical analysis of the amplification of pressure waves in two-phase combustion systems. The most recent work in spray detonations was conducted by Ragland, Dabora, and Nicholls at the University of Michigan.[17] They extended Williams[13] analytical treatment by relaxing a number of his assumptions. A listing of these analytical expressions and their homogeneous counterparts can be found in their report[17] where it is shown that if the sprays are sufficiently dilute, that is, if the volume fraction of liquid to gas is much less than one, one can use the familiar homogeneous detonation relations to calculate the detonation pressure ratios and velocities. Whether or not the liquid volume fraction in these engines at the time of ignition satisfies these requirements remains to be determined; however, until this information is available, it will be assumed that the homogeneous detonation relationships can be applied.

In experiments using diethylcyclohexane--oxygen mixtures and a 2-inch id by 8-foot steel pipe, Ragland et al,[17] measured maximum detonation velocities of about Mach 5 (5,300 to 5,700 feet per second) and pressure ratios of 30 to 1. These values are lower than their theoretical values of 7,850 feet per second and 45 to 1 for the velocity and pressure, respectively. The latter value is probably in error because the calculation neglects the finite extent of the reaction zone which may be appreciable for sprays. Extending the reaction zone behind the leading shock relaxes the coupling between the shock and the combustion zone and consequently lowers the pressure ratio. These results suggest that the analytical calculations of spray detonations based on this model overestimate both the detonation velocity and pressure ratio.

Using these values to estimate deflagration and detonation pressure ratios in the 100-lb thrust hypergolic engines, it was assumed that: (1) the propellants enter the combustion chamber at the rate of 150 grams per second (0.33 pounds per second), (2) ignition is delayed 5 milliseconds, and (3) all the injected propellant is retained in the engine, resulting in an accumulation of 0.75 grams of the mixture prior to ignition.

From the previous discussion it can be seen that, if the volume of liquid to gas in the heterogeneous mixture is negligibly small, the detonation parameters are dependent solely on the mass concentration of propellant mixture, whether liquid or gas. The entire mass of propellant can then be converted to gas at constant chamber volume before making the calculations. Thus we find that 0.75 grams of propellant mixture yields a gas pressure of about 3.7 atmospheres in these 100-cc-volume engines. For a constant volume deflagration the pressure should increase by a factor of about 8 or 400 psia. The detonation pressure ratio, however, for the N_2H_4/N_2O_4 system initially at 25°C is about 15 to 1, giving a detonation pressure of 55.5 atmospheres. Multiplying this by 2.5 (2 to 2.5 are the usually accepted factors to account for reflection from the chamber walls), yields a total reflected detonation pressure of 140 atmospheres or 2,100 psia; this compares with a reflected detonation pressure of 600 psia corresponding to an initial chamber gas mixture pressure of 1 atmosphere. In view of the maximum values used in the calculation, both the deflagration and detonation pressures have been over-estimated. Considering the fact that Ragland et al, measured detonation pressure ratios approximately 30 percent lower than the theoretical value (apparently due to the extended reaction zone of heterogeneous detonations), it appears that this value might also be larger than the real value, and, in fact, it may be 70 percent as large or 1,500 psia.

In studies conducted in 1952, Loison[18] demonstrated that pipes having their interior surfaces covered with a thin film of combustible liquid and filled with oxygen could support stable detonations when initiated by shock waves of suitable strength. Similar studies were also conducted by Gordeev, Komov, and Troshin[19] in 1965; they used oil films and oxygen which were initiated by methane-oxygen detonations, lead azide, or exploding wires. Ragland et al,[17] conducted similar but more extensive studies using diethylcyclohexane films and oxygen in glass pipes. They measured detonation velocities and pressure ratios of 3,750 feet per second and 17 to 1, respectively, considerably below the values obtained for the sprays. High speed photographs of these detonating film-gas systems showed that the combustion process occurs in the boundary layer in the wake of the shock wave. This would explain the low values observed for the detonation pressure and velocity since the coupling between the combustion zone and the shock front would be weaker than for the spray detonation. By applying these results to the rocket engines, one finds that when the effect of the combustion of the Aerozone-50 coolant film covering the chamber's interior walls is included, the calculated detonation pressures increase from 2,100 to about 2,500 psia. It appears from this discussion that ignition pressure spikes as large as 2,500 psia, although rare, could be generated by heterogeneous detonations, whereas, deflagrative combustion of this same heterogeneous system results in combustion pressures smaller than 500 psia.

If both types of combustion processes (detonation versus deflagration) occur in the engine, one would expect to find a binormal distribution of the pressure spikes; the mean pressure spikes corresponding to deflagration

($<$ 500 psia) and detonation ($\sim$ 2,000 psia in reflection) should be separated by a factor of at least 2, and the factor should be greater when considering the wide differences in burning velocity. However, such a binormal distribution in the pressure spikes has not been observed.

It has been shown that by assuming the existence of heterogeneous detonations one can account for reflected pressure spikes as large as 2,500 psia. However, it is not yet clear how such detonations originate. If one assumes that the combustion starts with a thermal ignition (representing a soft ignition) in the gas phase, the initial flame kernel would be deflagrative since a shock front is not initially present; in the case of strong electric spark ignitions a shock wave is created, and it is conceivable that this wave and the chemical reaction couple to create a detonation. Since this is not the case for thermal ignitions, however, the combustion process itself must somehow create the shock in order to transit to a detonation.

There are currently two theories concerning the transition of a deflagration to a detonation. One theory maintains that acoustic waves generated by a propagating, and preferably, accelerating deflagration culminate in a shock wave that heats the reactants immediately behind it to their ignition temperature and the shock wave followed by this deflagration, form a detonation. In the other theory it is believed that the original deflagration eventually merges with the shock it created (this is possible since the deflagration always travels in the compressed gases behind the shock) forming a detonation. Both of these mechanisms require a finite distance of travel before a detonation can form; usually this "induction" distance is some function of the vessel size and geometry. Stern, Laderman, and Oppenheim[20] have recently studied the acceleration of flames in detonable gas mixtures initiated by hot wires. Similar studies, previously conducted by Bollinger and Edse,[21] using 2-inch diameter by 6-foot long cylindrical pipes, showed that several feet of deflagration travel in a stoichiometric hydrogen-oxygen mixture was required for the combustion process to attain a stable detonation, although no sharp demarcation separated the two. By extrapolating their results to lower velocities, it was found that the flame front attains speeds greater than sonic (300 meters per second) after approximately 1 foot of travel in the apparatus. The nature of the flame acceleration process depends on numerous factors including the mixture temperature, pressure, homogeneity, turbulence and the size, geometry, and condition (roughness) of the confining vessel. A complete discussion of these parameters is beyond the scope of this report. In general, it has been found that chambers whose diameter-to-length ratios are about one, exhibit oscillatory, but not detonative, combustion. On the other hand, turbulence, which is certainly present in these engines, tends to shorten detonation induction distances, while the presence of droplets increases them. Based on the results of previous studies one might anticipate that ignition in these engines, if thermal in nature, should not transit to a detonation within the engine volume. However, the previous investigators were concerned with quiescent systems having simple vessel

geometries. The turbulence and heterogeneity of the system in combination with the velocity gradient in the convergent section of rocket engines provide an effective increase in the engine length, particularly for flames originating in the vicinity of the throat.

As can be seen, there exists a number of possible modes for the formation of heterogeneous detonation, however the problem is to determine which, if any, of these various possibilities contribute to detonation.

Condensed Phase Combustion: Three types of condensed-phase material apparently accumulate on the interior walls of the engine combustion chamber: (1) frozen mixtures of the propellants, (2) unmixed liquid deposits of the propellants, and (3) products of preignition or post combustion reactions. It is conceivable that any or all of these materials could be contributing to the hard start phenomenum. Since it is now known that all of these systems exhibit explosive characteristics the possibility of any one contributing to the hard start problem cannot be overlooked.

During the early stages of the engine pressurization, frozen mixtures of each of the propellant fuels, N_2H_4, MMH, and UDMH, in combination with N_2O_4 are formed when the chamber pressure is sufficiently low that vaporization of the liquid freezes the drops. The Bureau demonstrated that frozen stoichiometric mixtures of Aerozine-50/N_2O_4 and UDMH/N_2O_4 exhibit detonation-like combustion when their temperature exceeds -60°C. Similar mixtures of N_2H_4/N_2O_4 and MMH/N_2O_4 burned violently, but not detonatively, at this temperature. The mixtures studied were loosely packed, and as a result, the initial reactions dispersed the material, possibly preventing a detonative combustion. It is believed that increasing the packing density will increase the frequency of detonative combustion. Further reaction of these mixtures in heavy walled containers, such as a rocket engine combustion chamber, might provide sufficient confinement to initiate detonation. It is also believed, primarily from the experiments of Weiss,[22]/ that this violent reaction is a result of the thermal decomposition of a cryogenically unstable intermediate formed from the propellants at temperatures below the reaction point, although the exact nature of this intermediate has not been determined.

When frozen mixtures did not burn detonatively, a viscous yellow residue usually remained in the container following the reaction. Infrared analysis of the residue from the N_2H_4/N_2O_4 reaction showed it to be primarily a water solution of hydrazine nitrate, an explosive material.

The propellants used in these engines are stable materials not individually susceptible to detonation in either bulk or spray form. However, the presence of less than a few percent oxidant (O_2 or N_2O_4) in N_2H_4 sprays sensitizes the system so that it can support detonation-like combustion with an energy release equivalent to about 140 percent of that released by an equivalent weight of TNT.

In other experiments at the Bureau, liquid mixtures of these fuels when mixed sufficiently rapidly, with N_2O_4, burned explosively releasing energies equivalent to about 160 percent that of TNT, apparently, independent of the type of fuel used. Although TNT equivalences of the frozen mixtures were not measured, their values are believed to be similar to those of the liquid systems. From these studies it is apparent that explosions in the combustion chamber could conceivably originate from the combination of propellants.

It has been found, however, that propellants are not the only source of explosive reactions in these engines. Residues removed from MSC 100-lb-thrust $A-50/N_2O_4$ engines following altitude firings have been found to contain appreciable amounts of hydrazine nitrate (HN). In some cases the samples of residue removed were crystallized deposits of HN and, in others, water solutions of HN. Most of the latter solutions did not have a sufficient HN concentration to constitute a detonable mixture. However, these samples were removed from engines that had not spiked--a fact that may attest to their nondetonable nature. To support these findings studies were extended at the Bureau's Explosives Research Center using a two-dimensional transparent engine and the propellant combinations N_2H_4/N_2O_4, MMH/N_2O_4 and $A-50/N_2O_4$. In these studies it was determined that a chemical reaction occurred during the preignition period as evidenced by the deposition of a liquid residue on the chamber walls. The N_2H_4 and MMH systems formed wall deposits consisting of water solutions of HN and monomethylhydrazine nitrate (MN), respectively; $UDMH/N_2O_4$ formed predominately ammonium nitrate (AN) solutions and $A-50/N_2O_4$ formed an HN solution. Similar studies conducted by Seamans[23]/using the MMH/N_2O_4 combination also disclosed that MN is a major constituent of these residues.

Why ammonium nitrate is a product of the $UDMH/N_2O_4$ preignition chemistry rather than its fuel nitrate (unsymmetrical dimethyl hydrazine nitrate (UN)) has not been established. Ammonium nitrate was originally thought to be an intermediate preignition product, and it was assumed that this subsequently reacted with the fuel in the wall coolant film of the MSC $A-50/N_2O_4$ engine to form HN; however, since the Bureau's engine has no wall coolant film this theory looses much of its plausibility. In view of ammonium nitrate's relative shock stability compared with the fuel nitrates, the particular propellant combination $UDMH/N_2O_4$ should be less prone to exhibit residue detonation. From gas phase studies conducted earlier at the Bureau the remaining products of the preignition reaction appear to be N_2O, H_2O and N_2. Fortunately, the quantity of these nitrates deposited in the engine during a single pulse was found to be relatively small (<2 percent) compared with the theoretically possible amount. If this were the only mechanism of nitrate formation, it is estimated that, in the case of the N_2H_4/N_2O_4 engine, approximately 40 engine pulses would be required to accumulate 1 gram of the respective nitrate. Moreover, although it has not been established, it is believed that the majority of these nitrates are formed during the post

combustion period when considerably larger amounts of these propellants dribble into the engine from the emptying propellant manifold.

In addition to knowing when and how much nitrate accumulates in these engines, it is also essential to understand their combustion characteristics, particularly with respect to their detonability in the engines. In this regard Bureau investigators prepared the three fuel nitrates and studied their physical and combustion characteristics; ammonium nitrate has been previously studied by numerous investigators and its combustion character- istics are comparatively well established. One of these fuel nitrates, HN, has been of interest in explosive research for many years, primarily because it represents a smokeless explosive since its explosion products are only nitrogen and water. It was first prepared by Curtius and Jay[24] in 1889 and has subsequently been studied by a number of investigators. Many attempts have been made to use HN as an constituent of artillery projectile propellants, and as a result, considerable information pertaining to its explosive properties has accumulated. HN exhibits two crystallographic forms; unfortunately, all the investigations to date, including those by the Bureau, have been confined to its beta form, and no information is available on the alpha form. These two forms probably have different explosive characteristics, as in the case with lead azide, which also has two crystalline forms.

One of the more interesting characteristics of HN is its relatively low combustion temperature, 2,400°C.[25] It is generally agreed that in bulk form the pure material decomposes explosively at about 300°C. However, in Bureau experiments using thin (0.1 inch) films of molten HN, it was found that HN could not be initiated to detonation by either flames, hot wires or jets of liquid N_2O_4, although it was previously established that such films of molten HN having thicknesses as low as 0.01 inches could support a stable detonation. Furthermore, solutions of HN and N_2H_4 having HN concentrations greater than 25 weight percent have been shown to support stable detonations in thin films. Aqueous HN solutions with HN concentrations greater than 70 weight percent are similarly detonable. It was also found that these films exhibit two detonation velocity regimes; a high velocity at about 2.5×10^4 feet per second and a low velocity of about 0.5×10^4 feet per second. It follows that the high velocity detonation will travel the 2-inch length of a 100-lb-thrust rocket engine combustion chamber in about 10 microseconds, the lower velocity taking about 50 microseconds. Comparing these times with the engine exhaust times of about 500 microseconds for a chamber gas temperature of 3,000°K, it is seen that the detonation combustion process is completed before the engine has had an opportunity to dump the detonation products. Shidlovoskii, Semishin, and Simutin[26] observed that molten HN contained in glass tubes did not support stable burning; apparently the combustion transited to a detonation. Moran, Burnett, and Smith[27] found that on heating vessels containing HN-N_2H_4 solutions, an explosive reaction occurred only after the liquid portions of the samples had either completely

burned or vaporized and the vessel temperature had risen to about 300°C. The infinite charge diameter detonation velocity of HN can be expressed as $V_D = 531\rho + 98.4$ meters per second,[28] where ρ is the explosive density in grams per cubic centimeter. The gap sensitivity of HN has been measured by Eyster, Smith and Walton[29] to be 50 percent greater than that of TNT, indicating that it is a relatively safe explosive to handle. Neither gap values nor detonation velocities have been obtained for MN or UN. Impact sensitivity experiments conducted at the Bureau established that these fuel nitrates are more sensitive to impact than ammonium nitrate. The order of increasing sensitivity appears to be AN, UN, MN, and HN. TNT equivalences, measured by the Bureau, are 142, 136, and 106 for HN, MN, and UN, respectively. Dwigging and Larrick[30] determined the detonable region for the ternary system N_2H_4-HN-water. While not particularly sensitive to detonation initiation, it is apparent from these results that the fuel nitrates (HN, MN, and UN) are relatively strong explosives.

Although there are still many questions to be answered concerning the properties of these materials, it seems fairly well established that their presence in rocket engines represents a hazardous situation.

Additional studies were made to determine the physical characteristics of these fuel nitrates. However, since they are not directly related to the spiking problem, a discussion of these results is presented in Appendix I.

IV. EXPERIMENTAL STUDIES

This section describes the various experimental studies investigated by the Explosives Research Center and problems related to ignition spiking and also discusses the pertinent work of other investigators.

The first section describes the studies to identify the nature and formation of the engine residues generated during low pressure pulse mode operation. The second section discusses the results obtained from studies concerned with the combustion characteristics of the propellants and the final section concerns the combustion characteristics of the fuel nitrates and related materials.

Two appendices are attached. One concerns the physical and thermochemical properties of the various fuel nitrates and the other, the structural and inertial response of small engines to internal explosions.

Materials: The N_2H_4, MMH, and A-50 used in these experiments were purchased in 5-pound quantities from Olin Mathieson Chemical Corporation at stated purities of 97.5, 98.0 and 98.2 percent, respectively. The UDMH, having a purity of 99.7 percent, was purchased from Food Machinery Chemical Company, and the N_2O_4 having a purity of 99.0 percent was purchased from the Matheson Company, Inc. Gaseous oxygen and nitrogen were purchased at 99.9

percent purity in compressed gas cylinders. Liquid nitrogen was supplied by the Linde Division of Union Carbide Corporation and was 99.99 percent pure. All of these materials were used as received, without drying or purifying.

The No. 8 detonator was a duPont product consisting of a copper alloy shell containing 0.20 grams of lead azide and 0.45 grams of PETN, sealed with a neoprene plug. The J-2 Army special detonator is a Hercules product consisting of a commercial bronze shell canister (3-inch long by 0.228-inch diameter) containing a main explosive charge of 0.94 grams of PETN. The tetryl pellets used in these experiments were pressed from tetryl powder into cylindrical pellets measuring 0.75-inch in diameter by 0.25-inch in height and weighed to the nearest 0.01 gram.

Engine Residues: Samples of residues collected by MSC personnel from their qualifying engines following firing at low pressure ($<$0.05 psia) were analyzed at the Bureau. The weights of the majority of the samples were less than one gram. The samples were first freeze-dried to separate the liquid and solid fractions. The liquid portion was always water clear and the solid was usually a straw yellow. The liquid portion was analyzed by gas-liquid chromatography using a 3-foot column of Carbowax 1540 at a temperature of 45°C. The solid portion was mixed with potassium bromide and pelletized for infrared analysis. Table 1 shows the composition of those samples received by the Bureau in satisfactory condition for analysis; several samples were either too small for satisfactory analysis or they were lost in shipment. These results show that, except for sample No. 24, water and HN were the major constituents of these residues. Later studies showed that none of the solution samples received had sufficient HN to constitute a detonable system.

Following these observations the Bureau completed construction of its 2-D transparent engine facility and experiments were conducted to determine the quantity of, and the time period of the pulse cycle during which the HN was being formed.

Figure 2 shows the essential details of the 2-D engine. The first study was concerned with investigating the preignition period. To avoid the usual post combustion reactions resulting from combination of the propellants following the closure of the propellant valves in the MSC engines, a piston displacement technique was selected for introducing the propellants. The pistons were made of teflon and separated the liquid propellants from the hydraulic driving fluid, which was usually water. An aluminum foil diaphragm and a teflon O-ring sealed the bottom of the glass lined propellant reservoirs. A hydraulic, rather than a pneumatic, line connected the high pressure driver gas (N_2) to the pistons to increase the system's response and avoid gross water-hammer effects. To insure reliable, simultaneous rupture of the aluminum diaphragms, it was necessary to use nitrogen driving pressures over 300 psia. Varying the pressure from 300 to 600 psia yielded fuel flow rates from 90 to 140 grams per

TABLE 1. - Composition of MSC Residues

Sample No.	Date Received	Origin of Sample	Residue/Distillate Weight Ratio	Distillate Composition (Analyzed by GLC[2]) Constituent Mole Percent		Residue Composition (Infrared Analysis) Weight Percent
10	6/6/66	Rocket nozzle	100/0[1]			HN > 90
12	7/12/66	Environmental chamber wall	58/42	Water Hydrazine Unknown	95 0 5	HN > 90
13	7/12/66	Cooling shroud	7/93	Water Hydrazine Unknown	98 0 2	Not enough residue recovered for reliable analysis
14	7/12/66	Rocket combustion chamber	100/0[1]			HN > 90
16	7/12/66	Injector face following run No. 59-22	100/0[1]			HN > 90
19	8/3/66	Residue taken 7-22-66 after 1000 pulses, origin Unknown	100/0[1]			HN > 90
24	8/19/66	Precup (after block 74)[3]	29/71	Water Hydrazine UDMH	93.0 4.5 2.5	HN >90 (Possible ammonium nitrate)

1/ Sample received as solid
2/ GLC-Gas-liquid partition chromatography
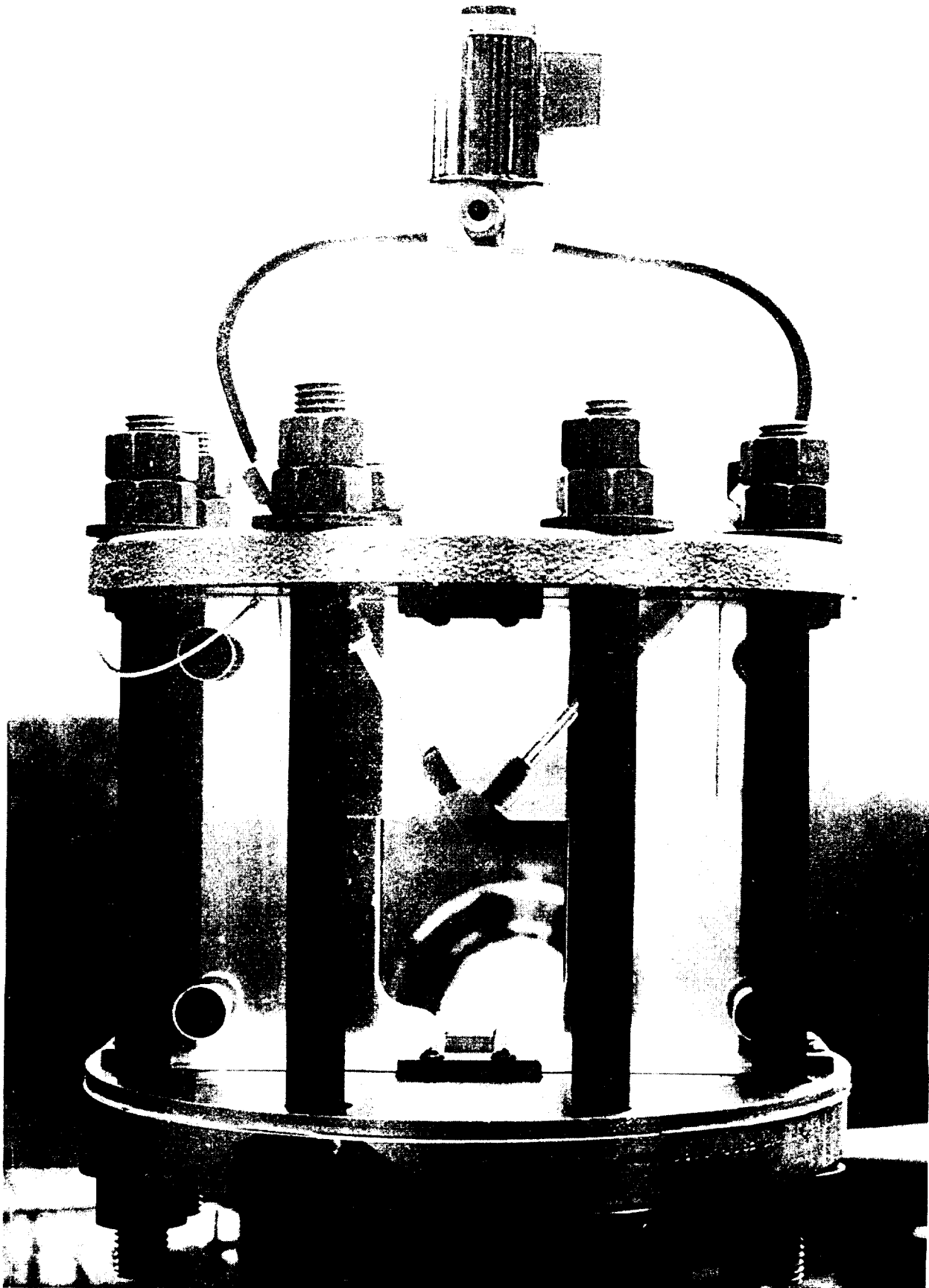3/ MSC test run designation

Figure 2:   2-D transparent rocket engine.

second and oxidant flow rates from 115 to 165 grams per second. Further adjustments in the flow rates were made by changing the diameter and length of the injector capillaries. A piezoelectric pressure transducer, flush mounted in the engine's wall, monitored the preignition pressurization process. The engine exhausted into a 67-liter evacuated (0.0002 psia) cylindrical vessel, whose volume was sufficiently large to insure that the flow at the throat remained sonic during the maximum anticipated time of propellant injection.

Although ignitions occurred in most of these runs, it was later found that they had no apparent effect on the results. The factors studied in the first investigation included the liquid injection rate, controlled by means of the N_2 driving pressure, and the fuel type. The F/O ratio corresponded to the stoichiometric value for each propellant combination.

A high speed framing camera operating at about 6,000 frames per second photographed the entire process including the motion of the teflon pistons. It was from these photographic records that the propellant flow rate was determined. The films showed that during the period of propellant injection a residue material was being deposited on the chamber walls. The pulse in general lasted approximately 5 milliseconds with ignition occurring at the end of the process. Following each experiment, a 0.1 milligram sample of the residue deposited on the engine walls, was removed for infrared (IR) identification. The remaining residue was washed from the chamber with distilled water and analyzed for total nitrate by the Nitron precipitation technique.[31]

The nitrates were identified by comparing the residue infrared spectra with that of previously synthesized material. These infrared spectra and the total nitrate analysis verify that the synthesized materials were in fact the desired nitrates of the respective fuels with purities greater than 99 weight percent. Figure 3 shows the IR spectrum of the various prepared fuel nitrates, AN, and the respective 2-D engine residues. The residues from the A-50/N_2O_4 combination had the same spectrum as those from the N_2H_4/N_2O_4 experiments. Table 2 shows the quantity and type of nitrates accumulated in the 2-D engine during a single pulse with this engine; the results are the average of four experiments. No evidence for

TABLE 2. -- Nitrate Accumulation in 2-D Engine
During Single Pulse

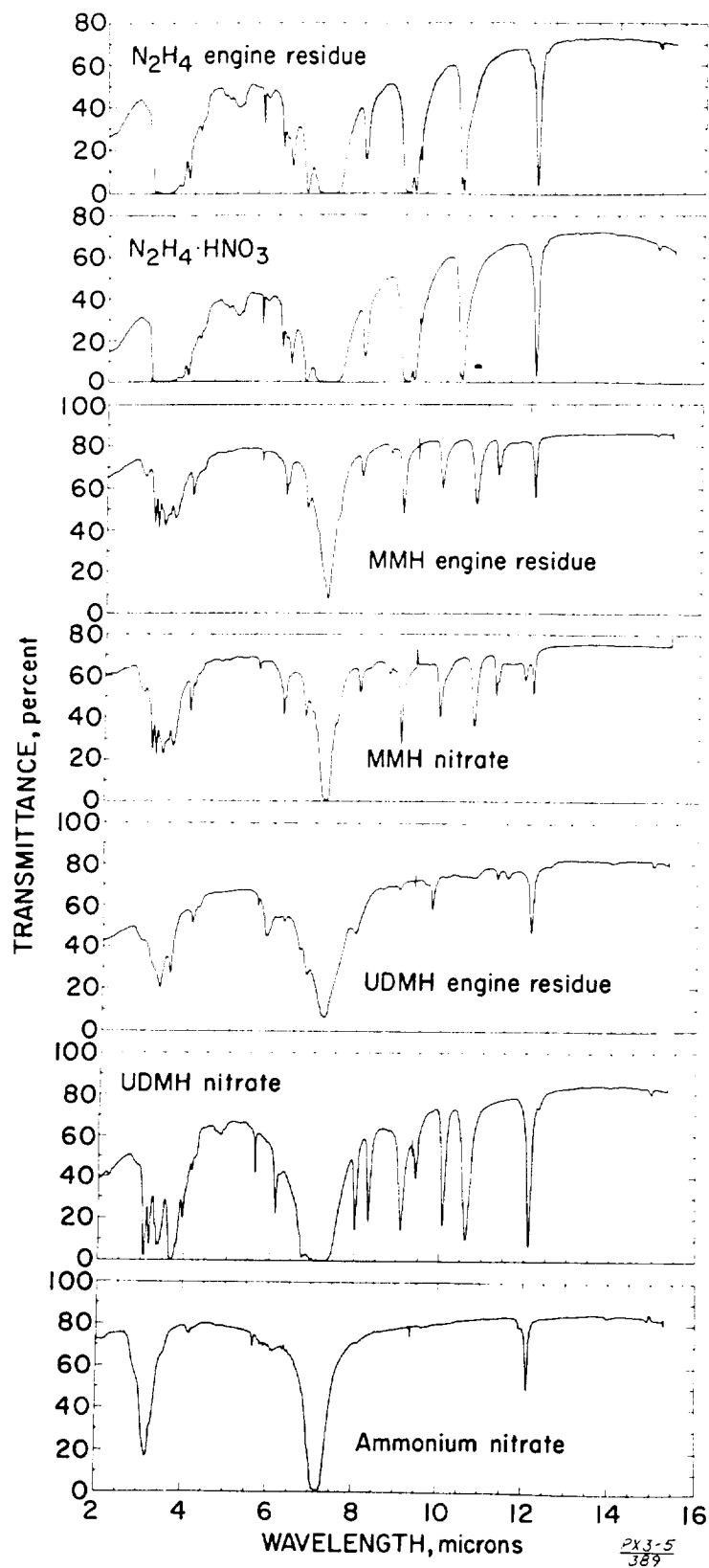| Fuel		Nitrate	
Type	Quantity (gm)	Type	Quantity (% Theoretical)
N_2H_4	0.5	HN	2.4
MMH	0.5	MN	1.2
UDMH	0.5	AN	1.6
A-50	0.5	HN	2.0

U.S. Gov't

Figure 3:   Infrared spectrum of residues and various
             prepared nitrates.

the presence of any parent fuel was found in any of these residues. Water appears to be the only other constituent of the residues in addition to the indicated solid.

It is interesting that the UDMH fuel forms primarily AN in the pre-ignition period with no evidence for the presence of UN, although both N_2H_4 and MMH form their respective nitrates. These findings agree with the results obtained in the low pressure vapor phase reaction conducted by the Bureau in 1961.[32/] Furthermore, the results for the A-50/N_2O_4 combination agree with those previously observed in the MSC engine residues, that is, that HN and water are the major constituents of these residues. On the basis of these earlier experiments, the absence of UN or AN was presumed to be due to the reaction of N_2H_4 and UDMH with the N_2O_4 to form AN which in turn reacts with the N_2H_4 in the A-50 wall coolant film, used in MSC engines, to form HN. Later experiments, however, established that although liquid N_2H_4 and AN react to form HN, UDMH and AN show no reaction, MMH reacts with AN to form an equilibrium mixture of AN and MN. In view of the results obtained (table 2) using the Bureau's engine which does not have a wall coolant film, it seems apparent that the assumption in the earlier experiments of AN as an intermediate loses much of its plausibility. This is particularly evident in the case of MMH/N_2O_4, because, if this theory applied, one would expect to find an equilibrium mixture of MN and AN resulting from the reaction of MMH and AN. Since this latter mixture has not been observed, it is concluded that AN is not an intermediate.

The fact that the fuel-nitrate (or AN) always deposits on the engine walls as a water solution and not as a solid suggests that the reaction occurs in the liquid phase of the jets and the products then diffuse to the walls, or the fuel deposits on the walls where it reacts with the N_2O_4 vapors forming the residue.

Table 2 shows only the total nitrate deposited on the engine walls. It seems reasonable that if the reaction occurs in the liquid phase of the impinging jets, the greatest portion of the nitrates is discharged out the throat; future experiments should determine this. It was also observed that the fuel-nitrate deposited on the chamber walls during the preignition period was not consumed or destroyed during the burn period of the engine pulse following ignition. Furthermore, the quantity of the nitrates that accumulates on the engine walls is very likely dependent on the engine and injector manifold geometry. Consequently, the numbers shown in table 2 for the 2-D engine used in this study, are not necessarily applicable to other engines having different manifold and engine geometries.

Propellant Combustion: The explosive potential of combustible materials is a difficult concept to determine a priori. Various techniques have been developed for determining the damaging potential of an explosive. In one of these, the work expended during the explosive decomposition of a known weight

of the candidate explosive is compared with similar work expended by an equivalent weight of TNT. This technique forms the basis of the ballistic mortar test used in the following studies in which the energy imparted to a projectile when fired from a mortar (figure 4) with TNT is compared to that fired with an equal weight of the candidate explosive. The absolute resolution of the ballistic mortar in these experiments is greater than $\pm$ 1 percent TNT equivalent at 100 percent TNT equivalent for 5-gram explosive charges. Because of its large time constant, this instrument cannot distinguish between a detonation and a deflagration; however its value to this study is the ability to simulate the conditions under which explosions occur in small rocket engines and to measure the maximum amount of work available from the explosion. Although there are other methods of defining TNT equivalence such as the blast wave technique, they are difficult to reconcile with destructive work in the rocket engine.

To perform an experiment the liquid samples and the detonator are sealed in concentric glass tubes which are then horizontally positioned in the firing chamber of the mortar. The 35-pound projectile is loaded in the mortar and the detonator is remotely fired and the recoil of the mortar to the explosive reaction is measured. Energy delivered to the mortar by the explosion is proportional to the energy released in the reaction, and the kinetic energy is equal to the potential energy of the mortar at its apogee. TNT equivalences of less than 10 percent for 5-gram samples are considered nonexplosive. The apparatus is calibrated by firing known weights of TNT. Two types of experiments were conducted using the liquid samples. First, the individual liquid propellants were fired in various atmospheres with a No. 8 detonator in the mortar; second, the various liquid fuels were fired with liquid N_2O_4 in an N_2 atmosphere under similar conditions. To obtain maximum energy coupling between the exploding detonator and the liquid, the detonator was placed under the liquid surface. To avoid contact between the copper-sheathed detonator and corrosive fuels, the detonator was capsulated in glass. Figure 5b shows the triple glass tube configuration used in the experiments requiring two liquids. Since the mass of the glass in these vessels affects the results, special care was taken to keep the weight of glass within desired limits.

The effect of the surrounding atmosphere on explosibility was investigated by purging the firing chamber with various atmospheres prior to firing the liquid samples.

Table 3 shows the results of the experiments conducted with 5-gram samples of the individual liquids using mortar atmospheres of N_2, air, O_2, and N_2O_4; each of these data is the mean of three consecutive experiments. No attempt was made to randomize the experiments, as it was previously established that the ballistic mortar was essentially drift-free. None of these liquids exhibit fast exothermic reactions when fired in a nitrogen atmosphere with a No. 8 detonator. However, when a J-2 detonator, containing a larger explosive charge was used, the N_2H_4 apparently underwent an explosive decomposition with an energy release equivalent to about 80

Power lead to control box

Support shaft

Knife edge and plate

Concrete support beam

29°

10' radius

Detonator
lead hole

Mortar

A

A

Inner liner

Front liner

Projectile

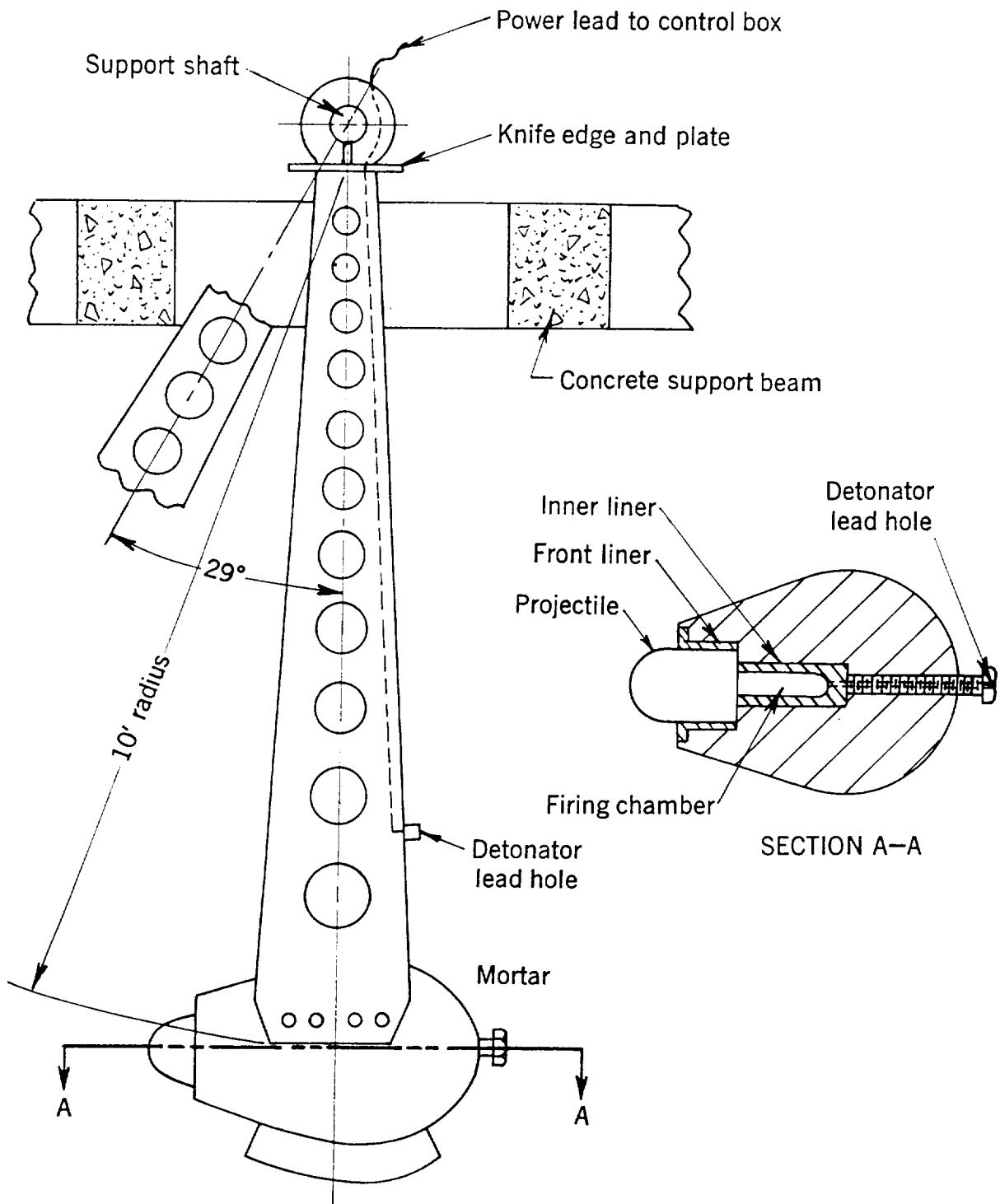Detonator
lead hole

Firing chamber

SECTION A—A

Figure 4:   Ballistic mortar apparatus.

PX3-103
554

percent TNT. The remaining liquids were not fired with the J-2, primarily because this represents an unrealistically large ignition energy, not likely to be found in the engines.

When the liquids were fired in air, O_2, and N_2H_4 atmospheres, only N_2H_4 appeared to give a large exothermic reaction.[2] However, it must be remembered that the O/F ratios for these shots were quite small since the oxidants had been added only to determine their effect on the reaction. Table 4 shows the calculated percentage of fuel consumed, assuming that the fuel and oxidant reacted stoichiometrically. Table 4 also shows the calculated TNT equivalence that would result from this reaction assuming an energy release equivalent to 100 percent TNT equivalence for the fuel-O_2 reaction and the largest TNT equivalent value given in table 5 for the fuel-N_2O_4 reaction. These results explain why Herickes, Damon, and Zabetakis[33] measured a TNT equivalence for liquid N_2H_4 in the ballistic mortar although they were unable to detonate the bulk liquid; the air in the mortar was contributing to the reaction.

The TNT equivalence of 140 for N_2H_4/air compares favorably with the value of 135 percent reported by Scott, Burns and Lewis.[3]

Table 3 shows that except for the A-50/N_2O_4 system when the other fuels are fired in air, O_2, and N_2O_4, the TNT equivalence is less than 10 percent, that is, below the limit of detection for this apparatus. For the A-50/N_2O_4 combination a mean TNT equivalence of 20 percent was obtained which is probably attributable to the presence of N_2H_4 in the A-50 mixture.

Although nitromethane did not detonate with a No. 8 detonator it is known to detonate consistently with a J-2 detonator under similar conditions. Liquid N_2O_4 was fired in a N_2 atmosphere in the mortar with a J-2 detonator because its heat of formation is positive it was thought that it might undergo exothermic reaction; however, the results indicated that no exothermic reaction occurred.

In the experiments in which liquid fuel and liquid N_2O_4 were explosively combined in the mortar, a coaxial arrangement of the glass tubes was used to provide maximum mixing (figure 5B). The innermost tube contained the No. 8 detonator and the two outer tubes contained the fuel and oxidant in the proper proportions to obtain a 5-gram stoichiometric mixture. To determine if the explosive yield is dependent on the position of the fuel and oxidant with respect to the detonator, both configurations were examined. Triplicate runs of the eight fuel/N_2O_4 combinations were randomized to minimize experimental error. The averages of the triplicate runs for each of these permutations are given as TNT equivalents in table 5.

Statistical analysis of the results showed that (1) the fuels had significantly different TNT equivalents and (2) placing the oxidant next to the detonator gave significantly higher TNT equivalents. The first result

TABLE 3. - <u>TNT Equivalences of Liquids Fired in Various Atmospheres</u>

Mortar Atmosphere	Propellants					
	N_2H_4	A-50	UDMH	MMH	N_2O_4	CH_3NO_3
N_2	<10	<10	<10	<10	--	<10
N_2 [1]	80 ± 20 [2]	--	--	--	<10	--
Air	140 ± 20	<10	<10	<10	--	<10
O_2	130 ± 20	--	--	<10	--	--
N_2O_4	150 ± 40	20 ± 10	<10	--	--	--

[1] J-2 detonator; in all other tests a No. 8 detonator was used.
[2] The confidence intervals represent 95 percent level of significance.

TABLE 4. - <u>Calculated Contributing TNT Equivalences of the Oxidation Reaction</u>

Fuel	Atmosphere					
	Air		Oxygen		N_2O_4	
	Fuel consumed, (%)	Contributing TNT equivalence	Fuel consumed, (%)	Contributing TNT equivalence	Fuel consumed, (%)	Contributing TNT equivalence
N_2H_4	1.5	4	7.4	16	14.8	65
A-50	1.0	2	6.1	14	12.1	50
UDMH	0.7	2	3.5	12	7.0	50
MMH	0.9	2	4.3	12	8.6	50
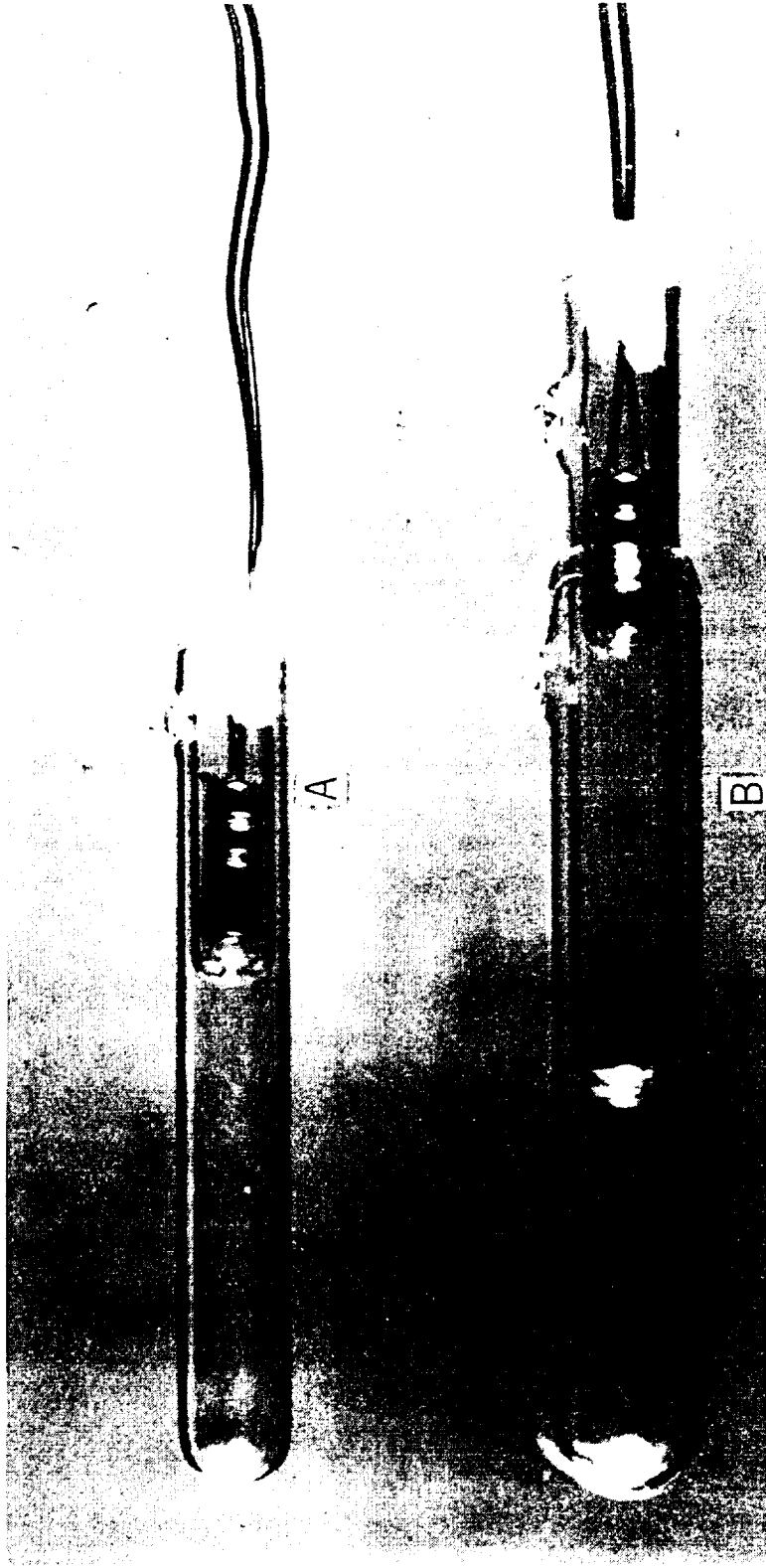
Figure 5: Glass assemblies for ballistic mortar experiments.

was expected. The second result indicates that the TNT equivalent depends on the concentric arrangement of the fuel and N_2O_4 and requires further study. According to the theoretical calculations of Willoughby, Mansfield, Goodale, and Wilton,[33] N_2H_4/N_2O_4 and A-50/N_2O_4 should have the same TNT equivalent and this is significantly lower than the corresponding maximum value shown in table 5. The value for A-50/N_2O_4, shown in table 5, is also considerably higher than that obtained by other investigators.[33] The only value close to the Bureau's is that of 90 percent TNT equivalence for A-50/N_2O_4 obtained in a deephole experiment.[33] These experiments show that, individually, except for N_2H_4, the fuels and N_2O_4 are to be considered non-explosive in either bulk or spray form, since they have been found not to exhibit a significant exothermic reaction. On the other hand, a hetero-geneous N_2H_4 system when initiated with a source equivalent to that of a No. 8 detonator in the presence of even small percentages of oxidant vapors, exhibits a violent exothermic reaction having a maximum TNT equivalence of about 150 percent. Very rapid dispersion and mixing of these fuels with N_2O_4 resulted in an exothermic reaction having a maximum TNT equivalence between 140 and 160 percent depending on the type of fuel. These results obviously support the hypothesis that heterogeneous mixtures of these fuels and N_2O_4 in rocket engines can support a violent exothermic reaction, probably a detonation.

TABLE 5. - <u>Measured Maximum TNT Equivalence for Liquid-Liquid Systems</u>

Fuel	Propellant adjacent to detonator	
	N_2O_4	Fuel
N_2H_4	155	148
MMH	139	90
UDMH	156	90
A-50	159	117

A study of the combustion characteristics of mixtures of frozen pro-pellants was also undertaken and it consisted of two parts: (1) an investi-gation of the thermal reactions using a differential scanning calorimeter (DSC) and small quantities of mixture, and (2) a determination of the detonability of larger amounts of these mixtures.

In principle, a DSC is a relatively simple device consisting of a programmed temperature controller which slowly raises or lowers the temperature of two small cells, one containing the sample and the other acting as a reference. The unit is purged with N_2 precooled with liquid nitrogen to remove water vapor. As the sample undergoes an exothermic or endothermic reaction, the DSC senses and compensates for any cell temperature difference

to keep the cells at the same temperature; the amount of energy added is monitored and recorded. Most commercially available apparatus are equipped with a dewar attachment for starting the experiments at low temperature.

For these experiments the DSC was calibrated with n-octane and tin. The average of three calibrations gave a melting point of -56.2°C for n-octane and +230°C for tin. These values compare favorably with the reported values of -56.5°C and +231.7°C, respectively.

The frozen propellants used in the various mixtures were prepared by slowly pouring liquid nitrogen into stirred liquid propellant, producing frozen particles somewhat smaller than ordinary table salt. The fuel and oxidizer were frozen in separate containers and stored under liquid nitrogen. Approximately 10 milligrams each of frozen powdered fuel and oxidizer were transferred to DSC sample cups and mixed at liquid nitrogen temperature. The cups were then quickly transferred to the DSC and following the establishment of thermal equilibrium, the DSC temperature programmer was started and the sample was warmed at a predetermined rate.

Figure 6 shows a typical DSC record for an A-50/N_2O_4 mixture. Point A in figure 6 marks the first indication of a slow exothermic reaction. At point B, a fast exothermic reaction occurs, corresponding to a vertical rise of the trace. At this point the thermal release rate of the chemical reaction exceeded the response of the DSC; in some cases using A-50/N_2O_4 mixtures gave an audible report similar to that accompanying explosive decomposition reactions. Following this fast reaction, the trace falls slightly and then rises again slowly to a broad peak before returning to the base line. When the DSC is opened at point C, a yellow liquid residue is observed in the sample cups, whereas when it is opened at point D no residue is visible. The liquid resembles that obtained from larger quantities of mixture. Although no infrared analyses were made, it is suspected that it consists of a water solution of HN which decomposes exothermically to generate the second peak. The frozen N_2H_4/N_2O_4, UDMH/N_2O_4, A-50/N_2O_4 and MMH/N_2O_4 mixtures all exhibited very similar thermal trace structures.

Table 6 lists the results of the thermal experiments for the various fuel/N_2O_4 mixtures showing the temperature at which the fast exothermic reaction occurs. Neither the flow rate of the N_2 purge nor the temperature scan rate of the DSC, which was varied from 2° to 20°C per minute, had any apparent effect on these values.

In other experiments using 1 to 100 grams of frozen fuel/N_2O_4 mixtures, similar to those in the DSC experiments, violent exothermic reactions occurred when the mixture temperature reached about -60°C. One out of 22 of these experiments with A-50/N_2O_4 gave a reaction with detonation-like characteristics. The other mixtures gave reactions that were accompanied by considerable fire and spewing of burning debris but no detonation. However, since these experiments were performed with loosely-packed frozen mixtures, it is conceivable
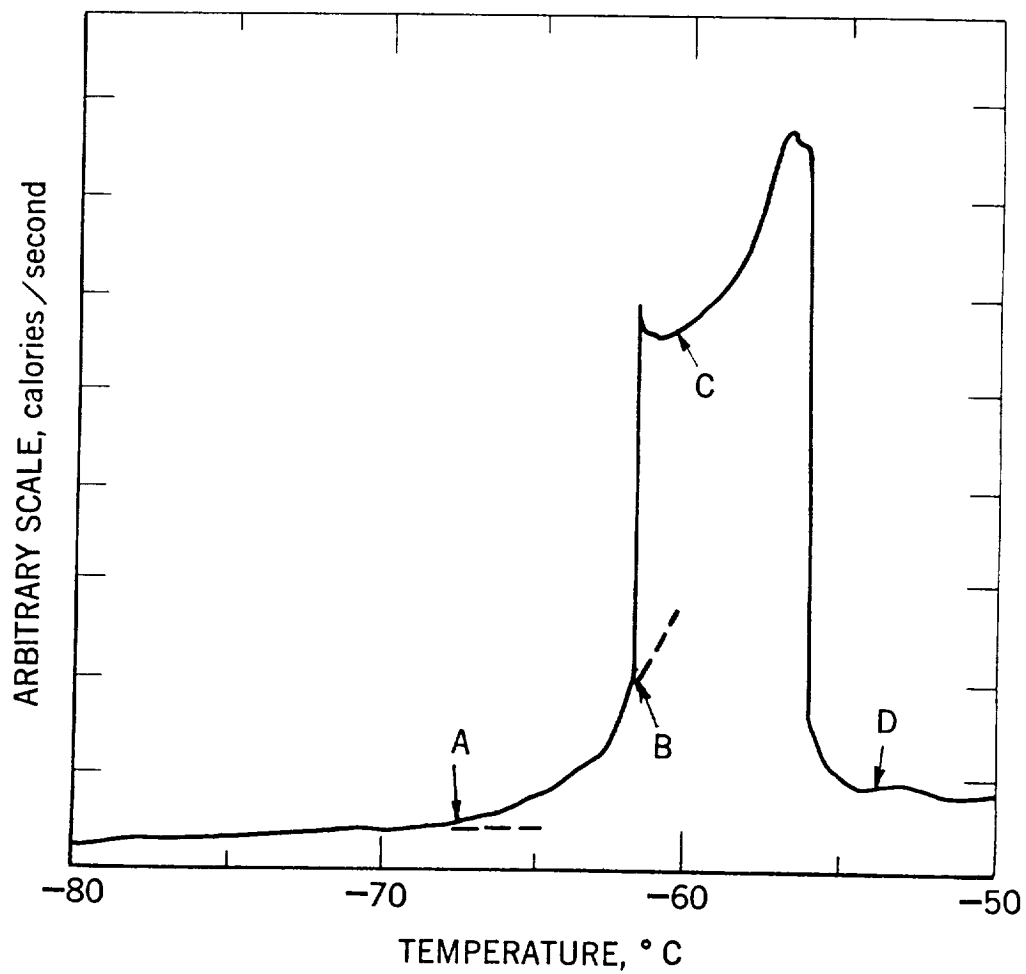
Figure 6: Differential scanning calorimeter record for an A-50/N_2O_4 mixture.

that increasing the packing density will increase the frequency of the explosive reactions. A yellow viscous residue often observed as a product of the less violent reactions was found by infrared analysis to consist primarily of a water solution of HN.

TABLE 6. - Temperature at which Fast Exothermic Reactions
Occur for Fuel/N_2O_4 Mixtures

Fuel	Number of runs	Fuel[1] melting point (°C)	Temperatures of fast reaction (°C)
N_2H_4	5	+1.5	-55+1
MMH	2	-52.4	-61+33 [2]
UDMH	5	-57.2	-60+7
A-50	5	--	-60+3

1/ N_2O_4 melts at -11.2°C.
2/ The large confidence interval is a result of limited sampling.

Residue Combustion: A final study was made of the combustion characteristics of the nitrate salts of the various fuels, (N_2H_4, MMH and UDMH). Of these, HN has been studied most extensively; AN has also been studied by many investigators, including the Bureau. A detailed account of these results is not presented, since AN is believed to be insignificant to the spiking phenomenum.

Both the impact sensitivity and TNT equivalences of the synthesized nitrates of N_2H_4, MMH, and UDMH were measured in the Bureau's standard impact apparatus. These results, shown in table 7 with similar results for AN, show that all the fuel nitrates are more powerful explosives per unit weight than TNT.

Additional work was done by Dwiggins and Larrick[30] to determine the detonability region of the ternary system HN-N_2H_4-H_2O. In these experiments metal cylindrical containers of various solutions were fired at one end with a 50-gram (1 inch by 1-5/8 inch diameter) tetryl pellet separated from the sample solution by a thin plastic sheet (0.002 inch). A witness plate was used to detect a detonation. In the event of a detonation a clean hole was punched in the witness plate, otherwise the damage was minor. Figure 7 shows the results of these experiments including the authors' data points. The figure shows that this ternary system has a large region of detonable compositions.
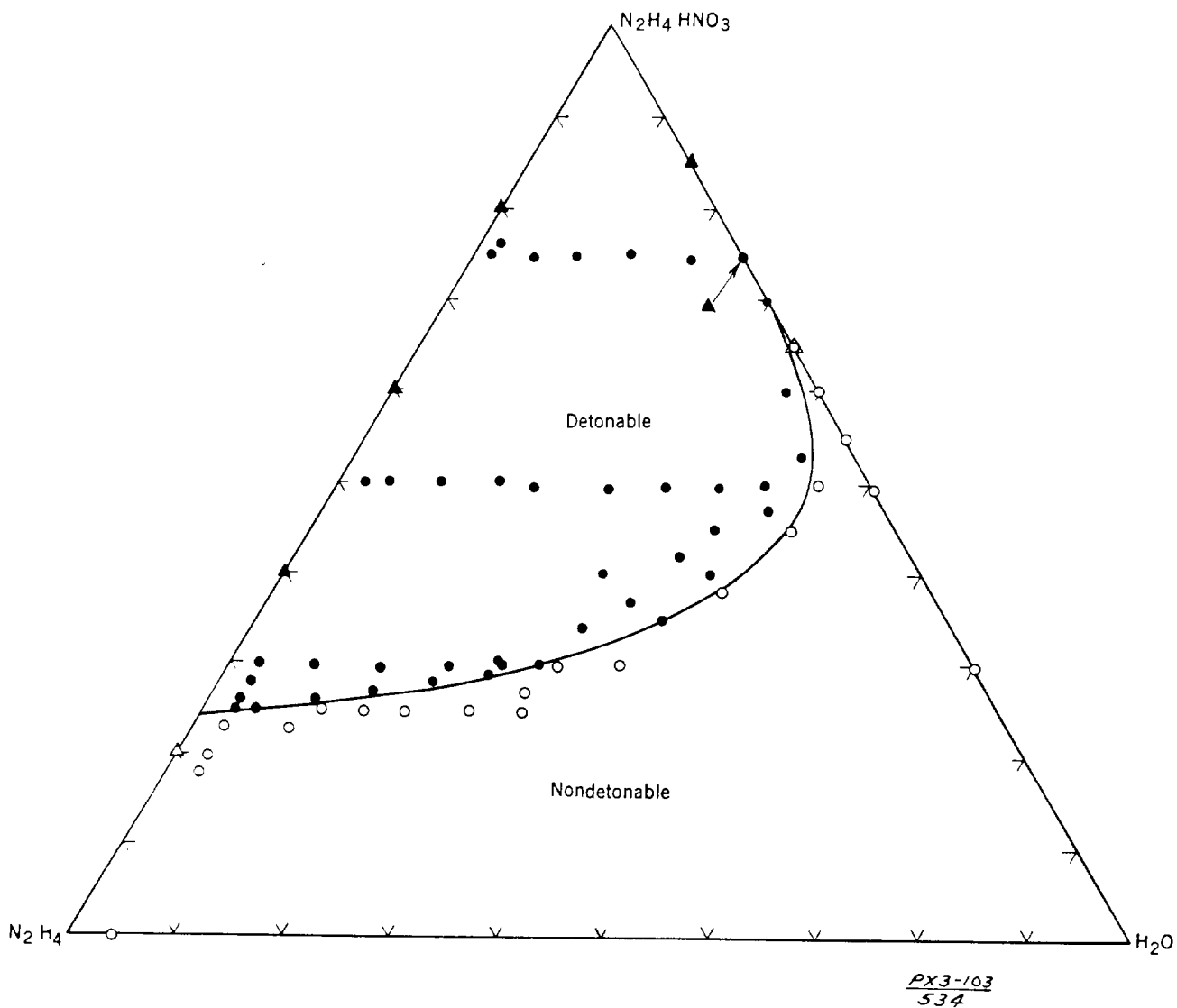
Figure 7: Detonation region for HN-N_2H_4-H_2O system at 25°C. The triangle data points correspond to the Bureau thin film results.

TABLE 7. - <u>Explosive Characteristics of the Nitrates</u>

	Melting point (°C)	Thermal decomposition temperature (°C)	Impact sensitivity (ft-lb)	TNT equivalence (weight percent)
HN	α:70 β:62	270	4	142
MN	40	235	6	136
UN	47	226	12	106
AN	164	230	119	79

The Bureau conducted experiments to determine the detonability of thin films of HN and its H_2O and N_2H_4 solutions, using the apparatus shown in figure 8, developed at the Bureau. It consists of an open plastic tray inclined at a slight angle so that the contained sample liquid forms a wedge whose thickness varies from 0.625 centimeters to zero. A collapsible probe[34/] extending the length of the wedge, was used to record the rate of propagation of the detonation front. This probe is a thin metal tube through which is extended a bare resistance wire separated from the tube by a spiral of insulating thread. As a detonation propagates along the tube, it collapses and shorts the resistance wire and the resulting change in the resistance is recorded on an oscilloscope. A resistive pressure gage[35/] located on the tray wall opposite the initiating explosive, provides a qualitative indication for the presence of a detonation. The explosive initiating charge consisted of a 50-gram tetryl pellet, 4.0 centimeters in diameter. The charge was separated from the tray wall by a plastic spacer which provides for the transmission of an attenuated shock into the liquid wedge. These experiments were conducted at 75°C with molten HN, HN-H_2O, and HN-N_2H_4 solutions. Figure 9 shows two oscilloscope records of the collapsible probe (lower trace) and the resistor transducer (upper trace) for a positive and negative result. The top oscillogram in the figure is typical of a positive result showing two detonation regions, a high and a low velocity. The high velocity detonation, conceived first, transits to a low velocity detonation when the film thickness reaches a critical value. The low velocity detonation then continues to its point of extinction at its critical film thickness. The upper trace in figure 9A is the output of the resistive transducer showing a strong shock striking it at the same time the low order detonation reaches the far end of the tray. Figure 9B shows the probe signal for a negative result (no propagation) for the 65 percent HN-H_2O solution. In this experiment the explosive shock was initially of sufficient intensity in the liquid wedge nearest the charge to collapse the probe; however, as the trace shows, this shock strength attenuated rapidly. Table 8 summarizes the results of the thin film detonation studies.
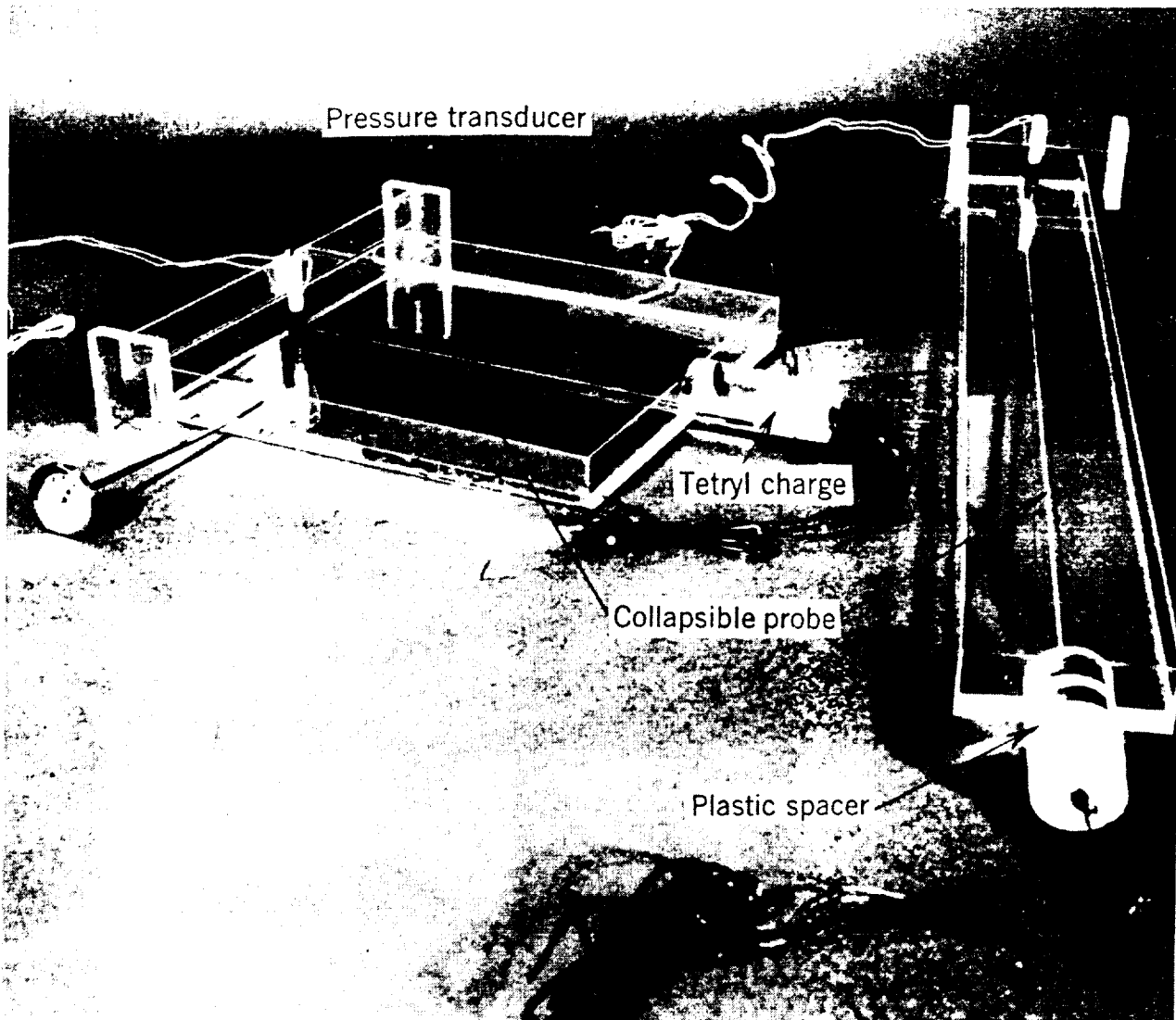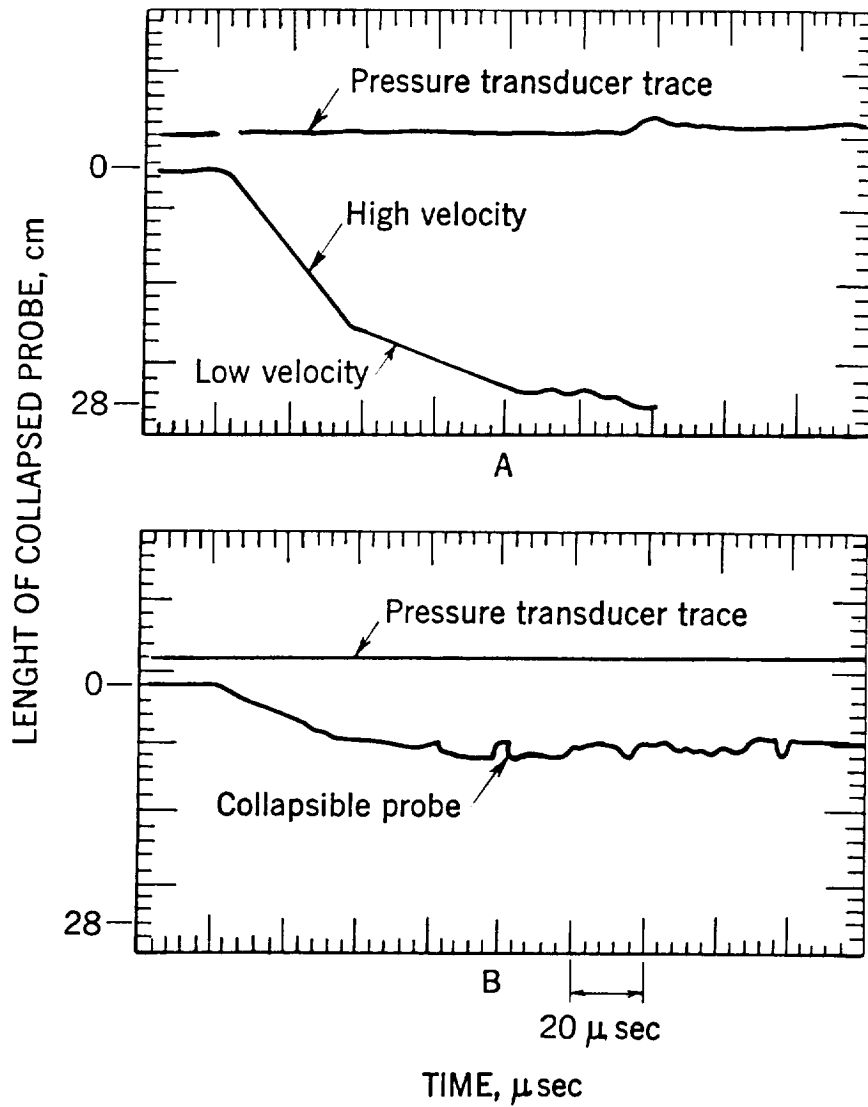
Figure 8: Thin film detonation apparatus.

Figure 9: Pressure transducer and collapsible probe records for a
detonating film (A) and nondetonating film (B).

TABLE 8. - Detonation Velocities and Critical Film Thicknesses (cft) for Both Low Velocity and High Velocity Detonations for HN-Water and HN-Hydrazine Solutions

Liquid Solution		Detonation Velocity			
		High Order		Low Order	
Composition	HN Concentration Weight Percent	Velocity m/sec	cft cm	Velocity m/sec	cft cm
HN	100	8,500	0.127	1,400	$\leq$ 0.025*
HN/H$_2$O	85	7,600	0.305	2,400	$\leq$ 0.025
	75	NOT OBSERVED		2,100	0.330
	65	NO PROPAGATION			
HN/N$_2$H$_4$	80	8,600	0.076	1,800	$\leq$ 0.025
	60	8,200	0.076	NOT OBSERVED	
	40	7,800	0.254	2,200	0.076
		NO PROPAGATION			

* 0.025 cm represents the limit of resolution of the apparatus.

From the table it can be seen that HN-H$_2$O solutions having 65 or less weight percent HN, do not support a stable detonation in thin films, whereas HN-N$_2$H$_4$ solutions with as little as 40 weight-percent HN still detonate. The table also shows that molten HN, HN-H$_2$O solutions with HN concentrations greater than 85 weight-percent, and HN-N$_2$H$_4$ solutions with HN concentrations greater than 80 weight-percent, exhibit stable detonation in films thinner than 0.025 centimeters.

The thin film detonation results are included in figure 7, where it is apparent that the binary mixture concentration limits for thin film detonability agree with the bulk solution values reported by other investigators. From this it seems reasonable to believe that results of the thin film and bulk liquid will be in accord for the complete ternary system.

Additional experiments were performed to determine if these films could be initiated to detonation by means of the various engine ignition sources. Three types were investigated: (1) forced injection of liquid N$_2$O$_4$ into molten HN; (2) hot body (thermal); and (3) flame. In the first study, liquid N$_2$O$_4$ was injected under the surface of molten HN by means of a hyperdermic syringe and needle. Although a violent reaction with flames occurred, the material did not detonate, and the fire subsided when the N$_2$O$_4$ flow stopped. In the case of the last two ignition sources the hot body was provided by an electrically heated nichrome wire, and the flame was supplied by a propane torch. In the case of the hot body, the molten HN burned only as long as the wire was red hot, but it did not transit to a detonation. Similar results were obtained for the flame. Directing the flame onto the surface of the molten HN did not appear to produce any noticeable reaction; however, heating the metal plate under the molten HN eventually resulted in a rapid, but nondetonative, combustion.

V. SUMMARY AND CONCLUSIONS

The nitrates of N$_2$H$_4$ and MMH were identified as constituents of MSC engine residues following low pressure pulsed engine operation. These nitrates are formed during the preignition period of the engine's pulse history, although it is suspected that larger amounts are generated during the post combustion period. Only about 1 percent of the theoretically possible quantity of HN and MN that can be formed during the preignition period remains in the engines after each pulse. AN was formed during the preignition period in engines using UDMH/N$_2$O$_4$. However, only HN and water were found in the residues of engines using A-50/N$_2$O$_4$. It is believed that detonation of the heterogeneous contents of the engine at the time of ignition can produce reflected pressure spikes as large as 2,500 psia; although this is not sufficiently intense to destroy the engine, repetition of this phenomenum could result in engine malfunction. Frozen A-50/N$_2$O$_4$ and UDMH/N$_2$O$_4$ mixtures were observed to detonate when heated to temperatures around -60°C. Neat hydrazine spray is relatively insensitive to explosion, although

the addition of small amounts of oxidant vapor appears to cause the system to burn explosively, yielding a TNT equivalence of about 140 percent. The remaining fuel sprays are not apparently sensitized by small additions of oxidant. Liquid fuel and liquid N_2O_4 react explosively, yielding a TNT equivalence of about 150 percent. The nitrates of hydrazine, MMH and UDMH are explosive materials having TNT equivalences of 142, 136, and 106, respectively, and decomposition temperatures of 270°, 236°, and 227°, respectively. Impact sensitivity studies show the order of increasing sensitivity to be HN, MN and UN. Liquid films of HN/H_2O and HN/N_2H_4 solutions having HN concentrations greater than 65 and 40 weight percent, respectively, can support a stable detonation. Both high velocity (7,600 to 8,500 meters per second) and low velocity (1,400 to 2,400 meters per second) detonations have been observed in these films. Molten HN and the more concentrated HN/water and HN/N_2H_4 solutions can support stable detonations in films as thin as 0.025 centimeters. The explosion of 10 grams of TNT in the center of a stainless steel 100-lb thrust engine is sufficient to rupture the engine walls and about 1 gram of TNT is sufficient to cause permanent damage. The damage resulting from such internal explosions depends not only on the charge weight but also on its location within the chamber.

APPENDIX I

Physical and Thermochemical Properties of the Fuel Nitrate

The HN, MN and UN used in these experiments were prepared by the procedure recommended by the Thiokol Corporation. Both infrared and total nitrate analysis indicated them to be over 99 weight percent pure. Their known physical and thermochemical properties are listed in table 9. As mentioned previously, two crystalline forms of HN exist. The beta form melts at 80°C with no apparent decomposition or sublimation. Robinson and McCrone[36] found that the resulting melt supercools readily and usually crystallizes as the alpha form. However, on seeding it with beta crystals, it reverts to the beta form at a rate which decreases with decreasing temperature. Due to the unstable nature of the alpha form, it is not possible to determine from the MSC residues which form is actually generated in these engines. No indication of any additional thermal (phase) changes in the crystalline structure of HN between -70°C and its melting point has been found; the system is therefore probably monotonic. These results agree with those obtained by the Bureau using a differential scanning calorimeter. Thermal studies of MN and UN made by the Bureau revealed no evidence for the existence of more than one crystallographic form.

Although all these nitrates are deliquescent, only the deliquescent properties of HN have been studied. Medard[37] conducted such a study using various Regnault mixtures (sulfuric acid of 11° Be′, 21° Be′, and 51° Bé) to obtain the various water vapor pressure environments. Figure 10, reproduced from Medard's report, shows his results; at 15°C HN absorbs moisture from an environment at 90 percent relative humidity at a rate of 0.01 gram of water per gram of HN per day. Unfortunately, Medard did not indicate the physical condition of the HN he used, and, obviously, the granular size and distribution are significant factors in this process.

Medard also examined the weight loss of anhydrous HN during intermittent heating to 110°C for a period of 315 hours (apparently the author attributes this weight loss to thermal degradation). He found this loss was linearly time-dependent, and amounted to about 8.3×10^{-5} weight percent loss per minute. Kissinger,[38] in similar work, found that the decomposition of HN at 130°C is "barely noticeable by the standard vacuum stability technique." He also reported that HN can be stored under 95 percent ethyl alcohol at a maximum temperature of 30°C for as long as four months without any "apparent ill effects." In similar experiments, using 20-milligram quantities of granulated HN (about the size of table salt), the Bureau measured weight loss rates of 3.0 weight percent per minute at 250°C, 0.4 weight percent per minute at 200°C, and 0.6 weight percent per minute at 150°C. Shidlovskii, Semishin, and Simutin[26] observed "an intense thermal decomposition of HN at 200-225°C and a flash at 270°C." This latter observation seems to agree with results obtained by the Bureau, in which impure HN decomposed explosively at about 270°C.

TABLE 9. - <u>Physical and Thermochemical Characteristics of HN, MN and UN</u>

Characteristic	HN	MN	UN
Formula weight	95.06	109.08	123.09
Density (x-ray), gm/cm^3	1.661	-	-
Melting point, °C	β:70.5	40.3	46.9
	α:62.5		
Heat of formation K cal/mole	59.8	-	-
Heat of fusion K cal/mole	4.56	4.47	4.31
Heat of solution K cal/mole	-8.72	-	-
Combustion temperature °C	2400	-	-
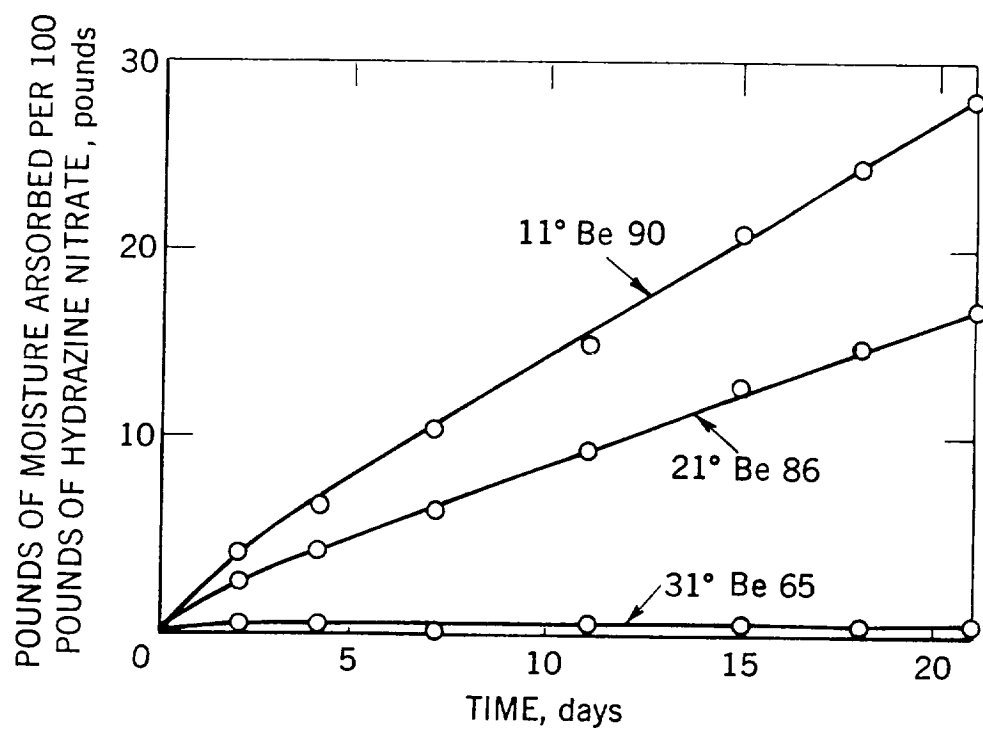
Figure 10: Weights of moisture absorbed per unite weight of HN
at various environmental humidities.

The solubility of HN in H_2O and in N_2H_4 has been studied by a number of investigators; among these Corcoran, Kruse, Skolnik, and Lieber[39] conducted the most extensive study. Their results for the three-component system $HN-H_2O-N_2H_4$ are shown in figure 11. The concentration triangular grid was not included in the figure to avoid obscuring the pertinent features of the phase diagram structure. The figure shows the isothermal contours for the liquidous surfaces of the ternary system and also shows that the system has four invariant points: two ternary eutectics, a ternary peritectic, and the eutectic of the quasi-binary system hydrazine hydrate-hydrazine nitrate 1-hydrazinate. Figures 12 and 13 show the liquidous lines for the $HN-H_2O$ and $HN-N_2H_4$ binary systems drawn from the results in figure 11. Figure 13 indicates the formation of the compound, hydrazine nitrate 1-hydrazine ($N_2H_5NO_3 \cdot N_2H_4$), which melts at $3°C$ and the eutectic composed of 47.5 weight percent HN which melts at $-46°C$. The data used to prepare these curves can be found in the authors' original papers.

Densities of N_2H_4 and HN/H_2O solutions have also been reported. Vango and Krasinsky[40] measured the density of two HN/N_2H_4 solutions containing a fractional percent of aniline. The Bureau also made such measurements using a 2-cm^3 pycnometer and a constant temperature water bath capable of holding its temperature within $\pm 0.5°C$. Figures 14 and 15 show the results of these experiments conducted at five temperatures between room temperature and $100°C$. Vango and Krasinsky's results are not included in these figures to avoid confusion; however, their values agree satisfactorily with those of the Bureau.

Viscosities of HN/N_2H_4 solutions were measured by Vango and Krasinsky[40] using a Cannon-Zhukov viscometer modified slightly to avoid evaporation or moisture pickup. Similar experiments on HN/N_2H_4 and HN/water solutions using a Cannon-Fenske viscometer were made by Bureau personnel. The kinematic viscosities of these solutions are shown in figures 16 and 17, where the kinematic viscosity is plotted as a function of the reciprocal of the absolute temperature. Although Vango and Krasinsky's data points are not included in these figures, their values agree with those of the Bureau.

Surface tension of HN/H_2O solutions at $25°C$ was determined by the Bureau using a DuNuoy tensiometer. These experiments were more difficult than anticipated, since it was found that the surface tension of freshly prepared HN solutions changed gradually with time. Even after standing several days in covered containers, the phenomenum did not appear to subside. Apparently, during the measurement the surface state of the solution was disturbed, and, as a result, the surface tension was lowered by each succeeding measurement. By careful preparation and filtration of these solutions, it was possible to obtain fairly consistent results. The values obtained by this method at a temperature of $25°C$ are given in figure 18. The figure shows a fairly linear dependence of surface tension on HN concentration.
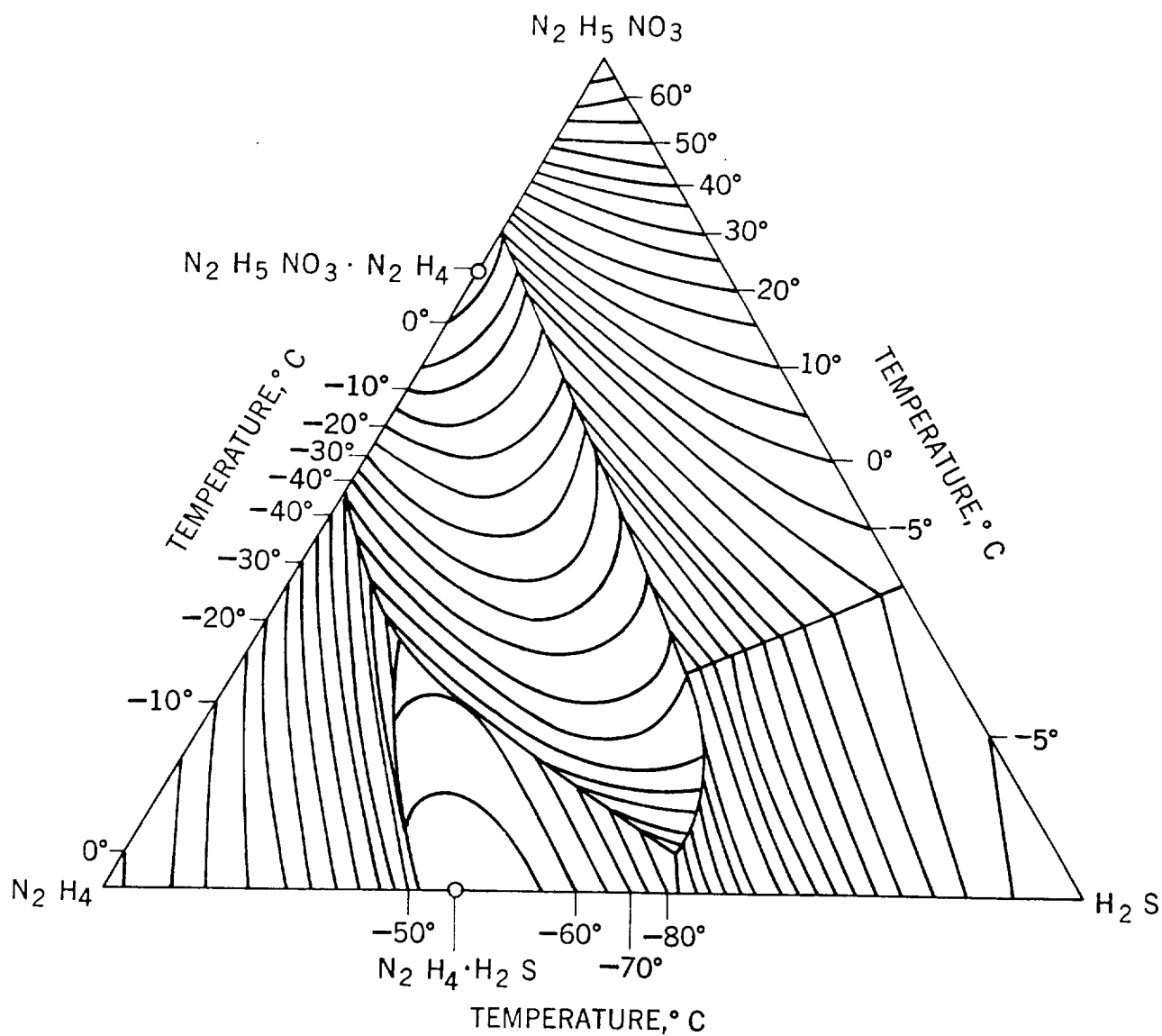
Figure 11: Ternary liquidous isothermals for the HN-N_2H_4-H_2O system.
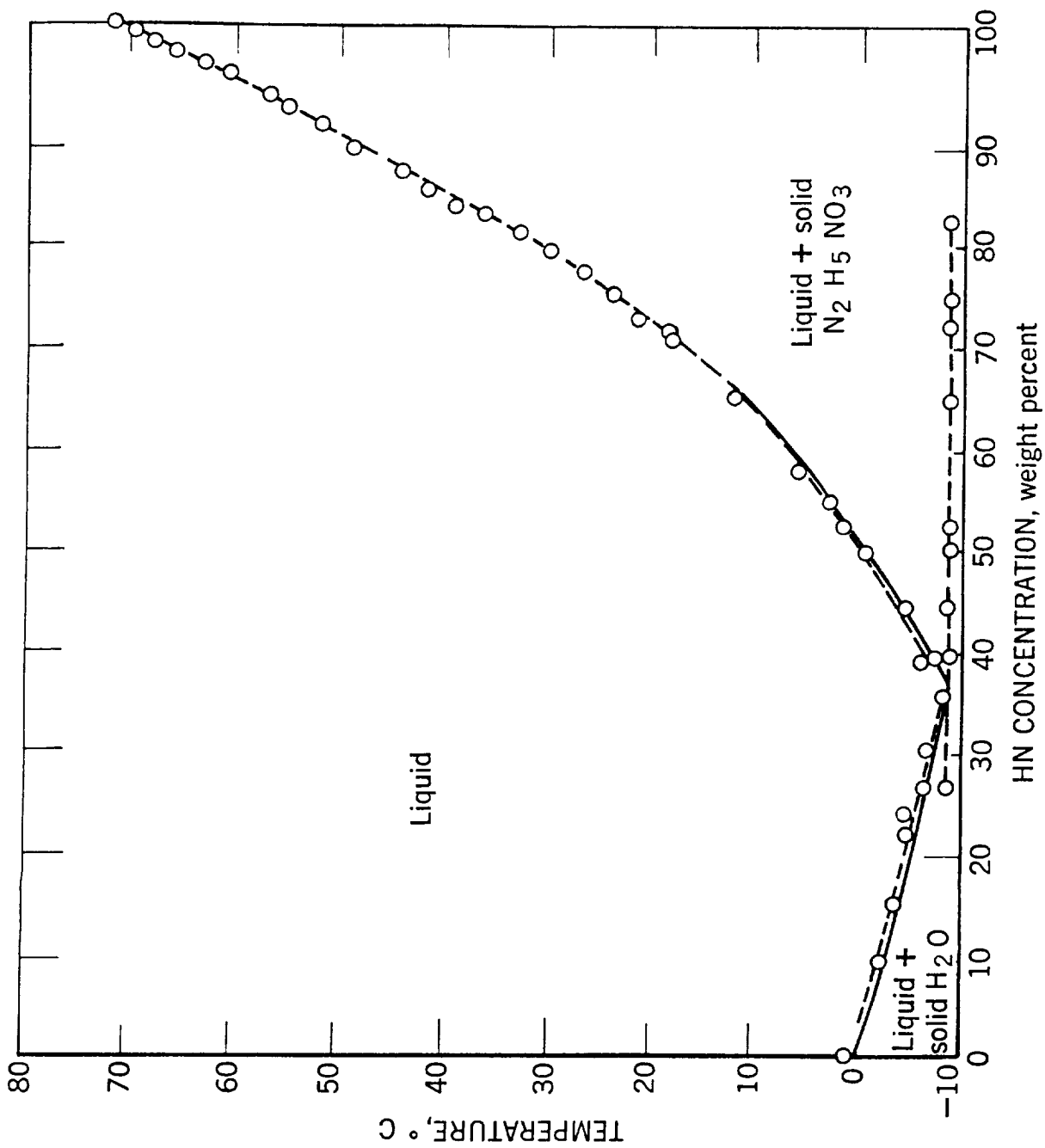
Figure 12: Liquidous line for the HN-H$_2$O system.

PX3-103
539
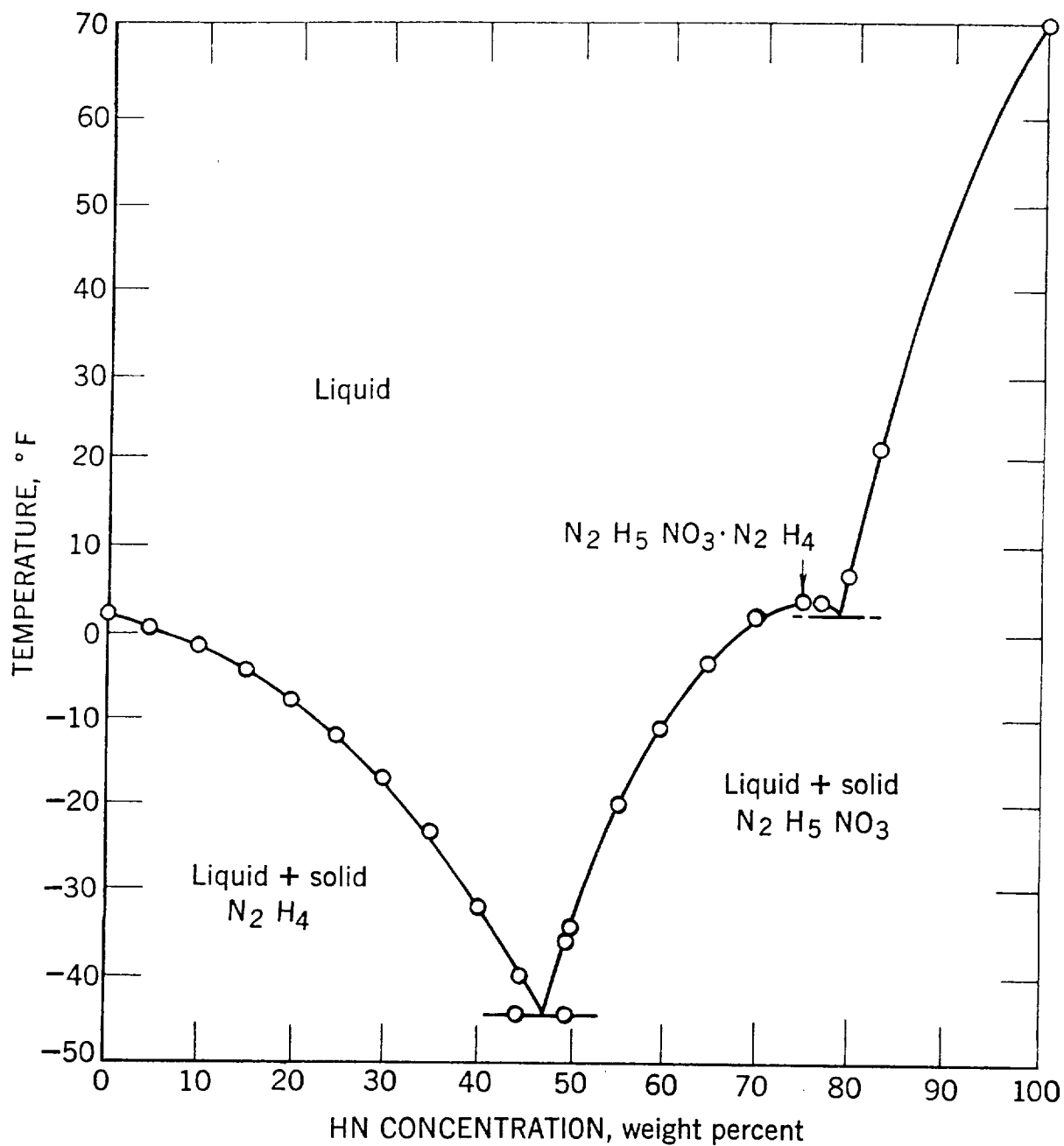
Figure 13: Liquidous line for the HN-N$_2$H$_4$ system.

The chart contains the following labels: TEMPERATURE, °F (y-axis); HN CONCENTRATION, weight percent (x-axis); Liquid; N$_2$H$_5$NO$_3$·N$_2$H$_4$; Liquid + solid N$_2$H$_4$; Liquid + solid N$_2$H$_5$NO$_3$.
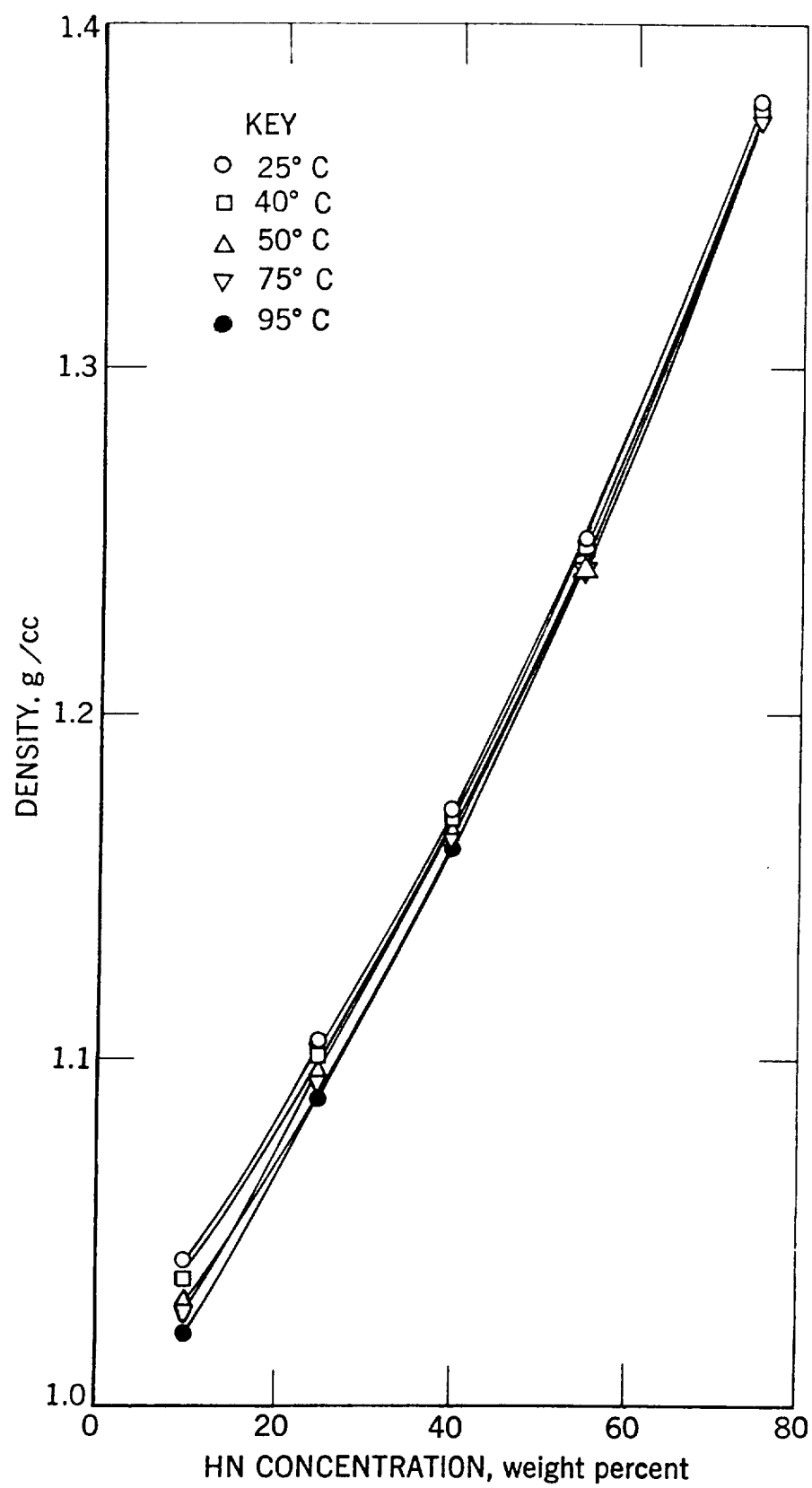
Figure 14: Density of HN-N_2H_4 solutions.
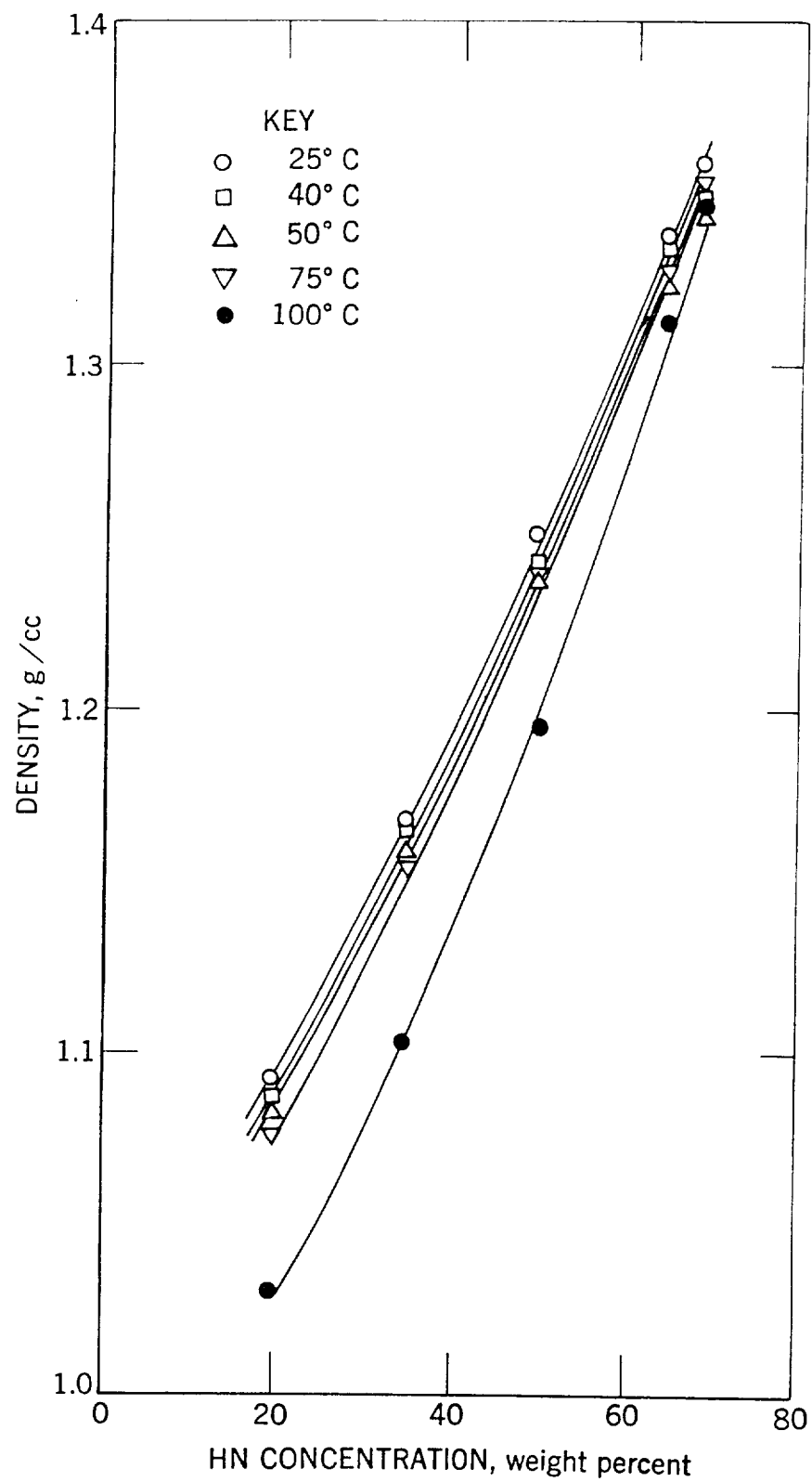
Figure 15: Density of HN-H_2O solutions.
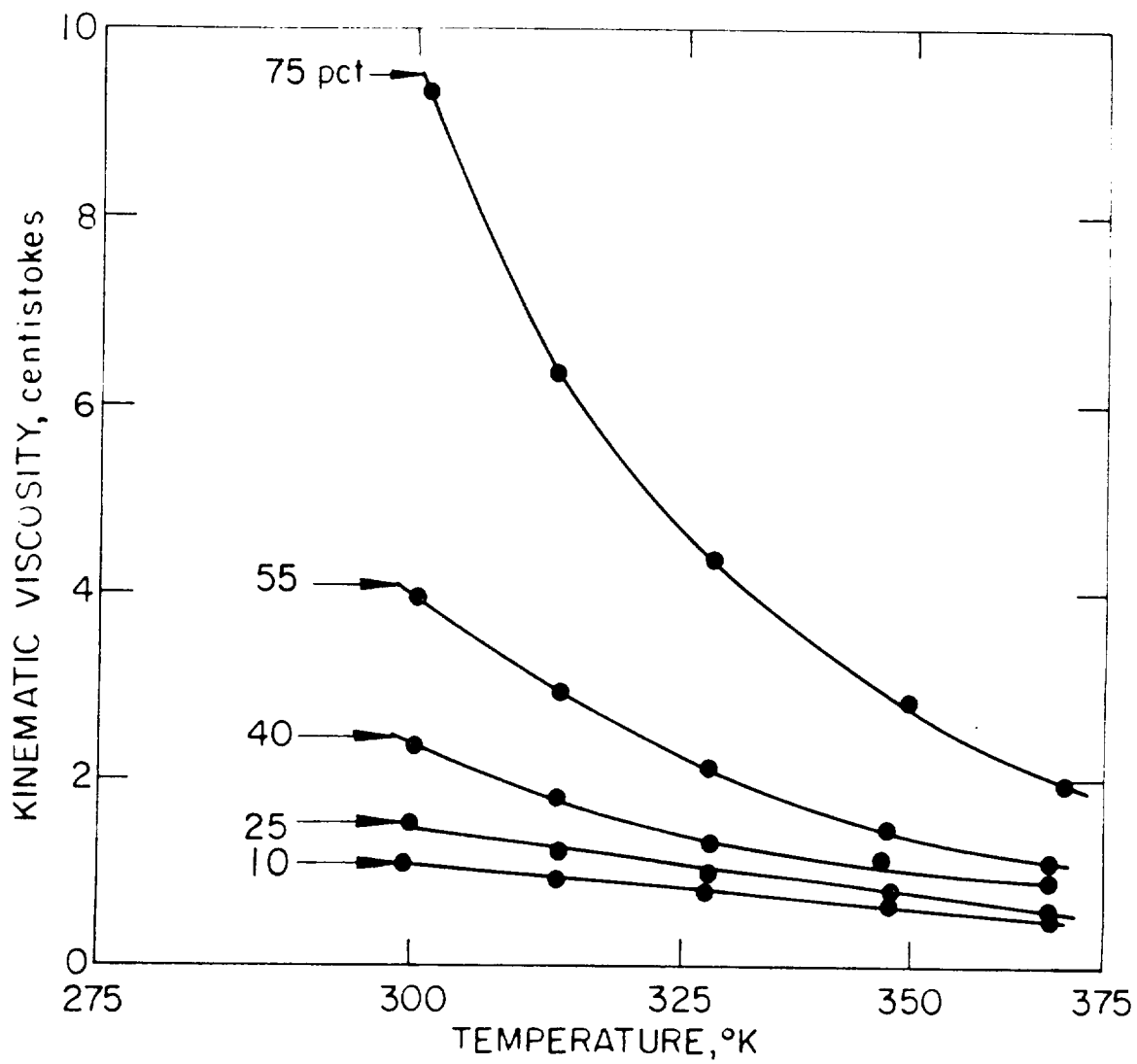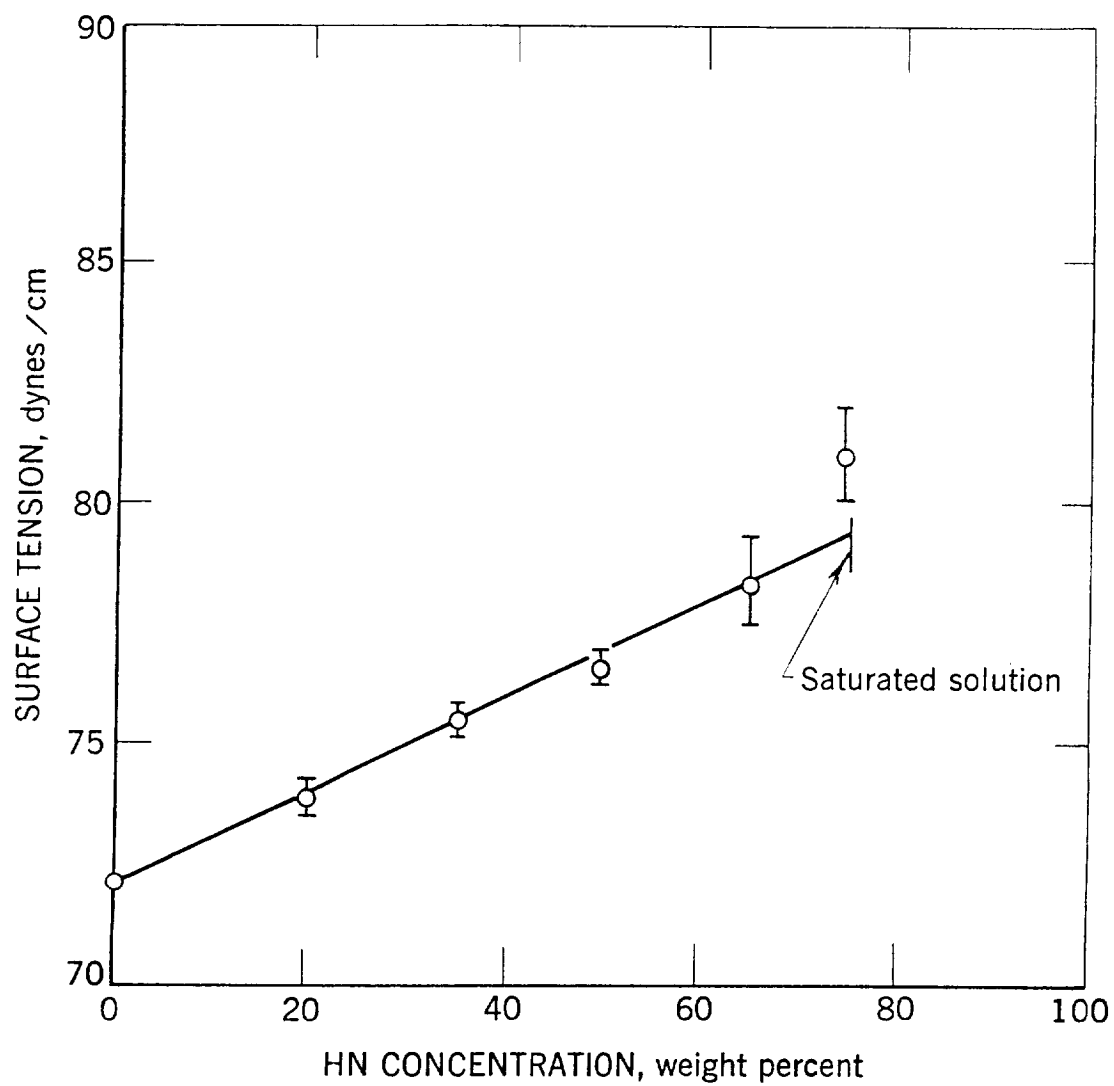
Figure 16: Kinematic viscosity of HN-N$_2$H$_4$ solutions.
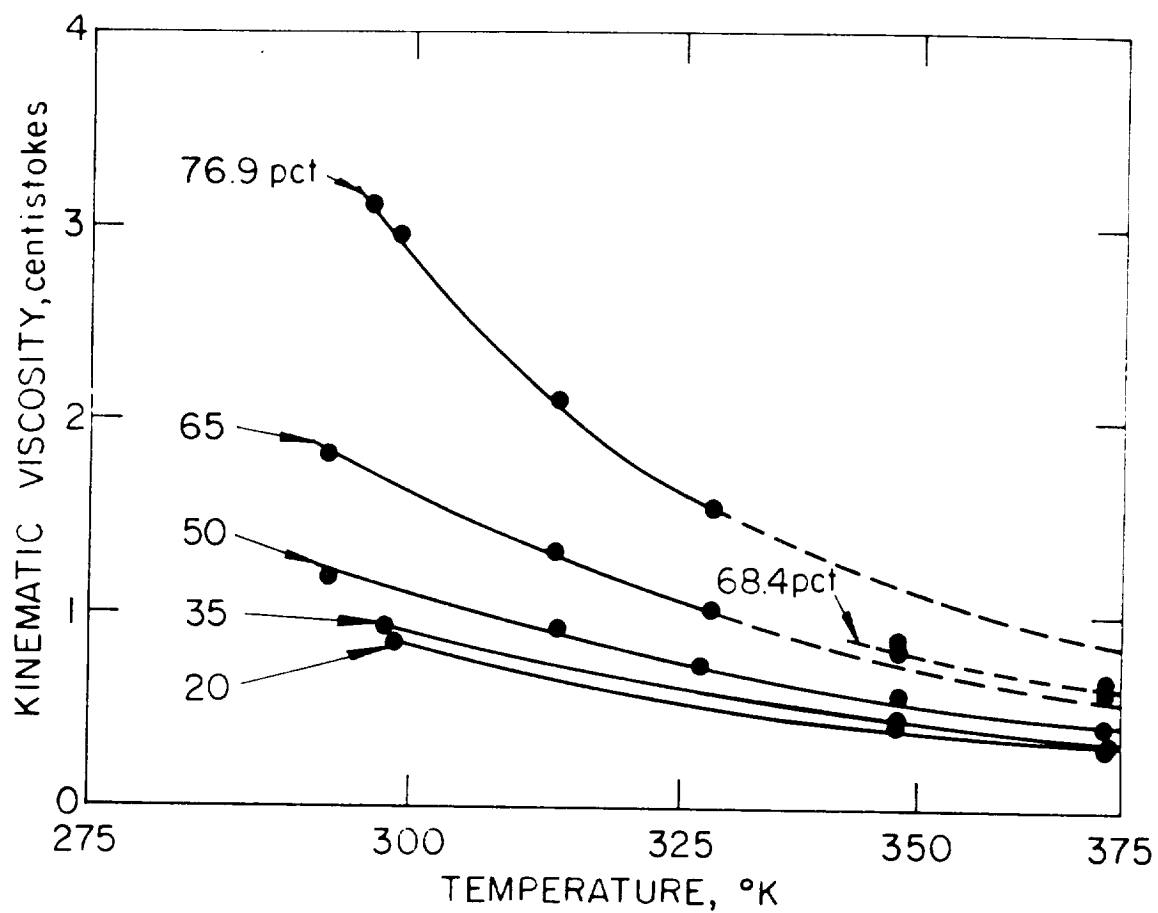
Figure 17: Kinematic viscosity of HN-H_2O solutions.

Figure 18: Surface tension of HN-H$_2$O solutions at 24°C.

PX3-103
547

In view of the difficulties encountered with this technique, it was decided to use another method for measuring the temperature dependence of the surface tension of liquid HN. The bubble technique[41/] in which a fresh surface is formed with each bubble was selected since it eliminates the drift problem. In principle this method consists of measuring the maximum pressure required to form a small bubble under the surface of the solution. The bubble pressure is proportional to the sum of the hydrostatic pressure and the ratio of the surface tension to the bubble radius. The apparatus was calibrated with liquids whose surface tension as a function of temperature was accurately known. A silicone oil bath was used to obtain temperatures up to 200°C. The surface tensions of molten HN, water and hydrazine were measured and the results are shown in figure 19.

Above 125°C molten HN begins to decompose noticeably as evidenced by the continuous formation of bubbles on the walls of the vessel. At 170°C the decomposition increased to such an extent that the liquid had the appearance of freshly poured carbonated water. The rising bubbles were so numerous that the liquid was almost opaque. As a result of the decomposition above 125°C, the surface tension measurements became noticeably erratic.

Vapor pressure studies of $HN-N_2H_4$ solutions containing a small percentage of aniline were made by Vango and Krasinsky[40/] and their results are shown in figure 20. The figure shows the normal logrithermic dependency of the vapor pressure versus the reciprocal of the absolute temperature.
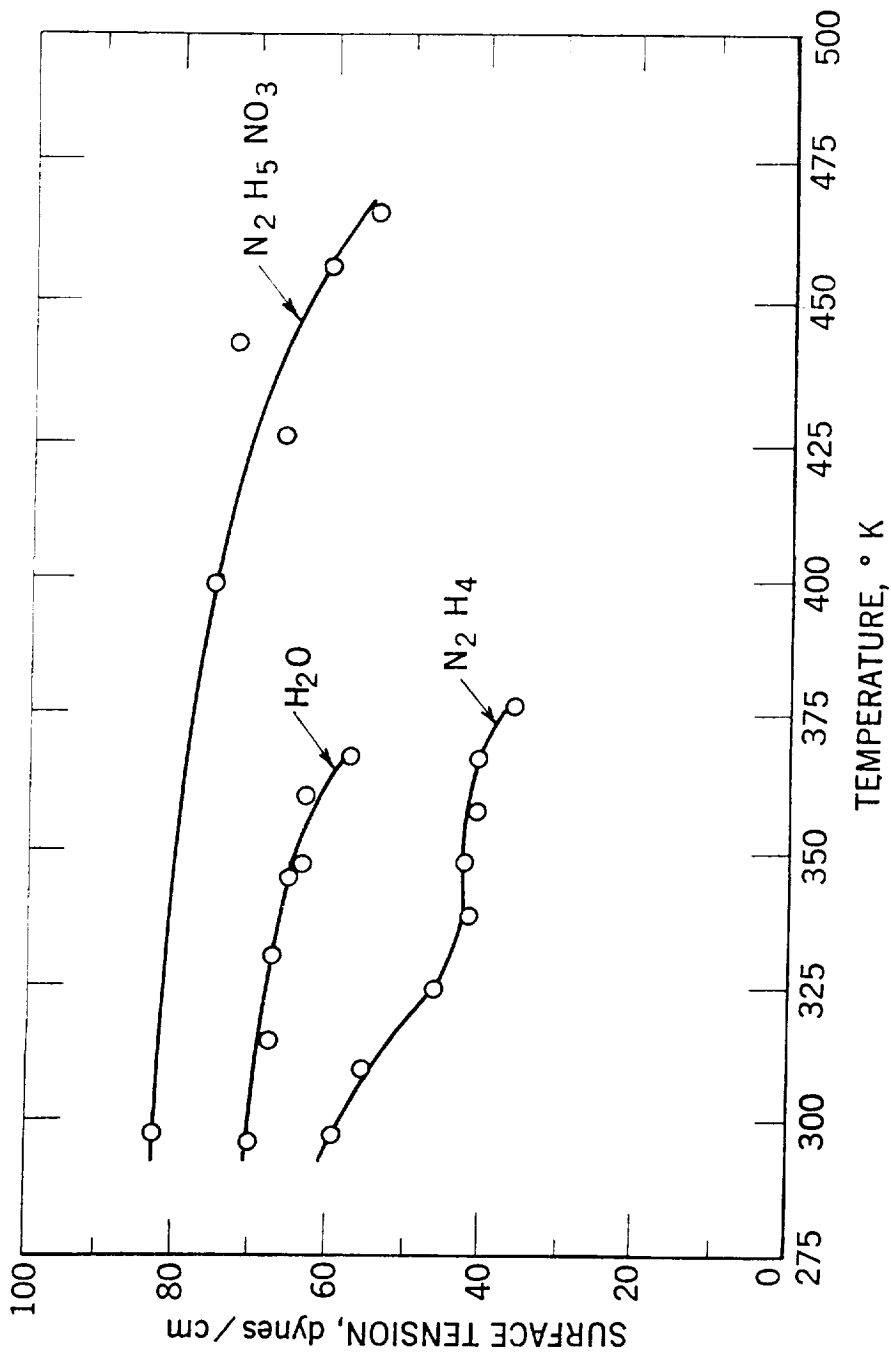
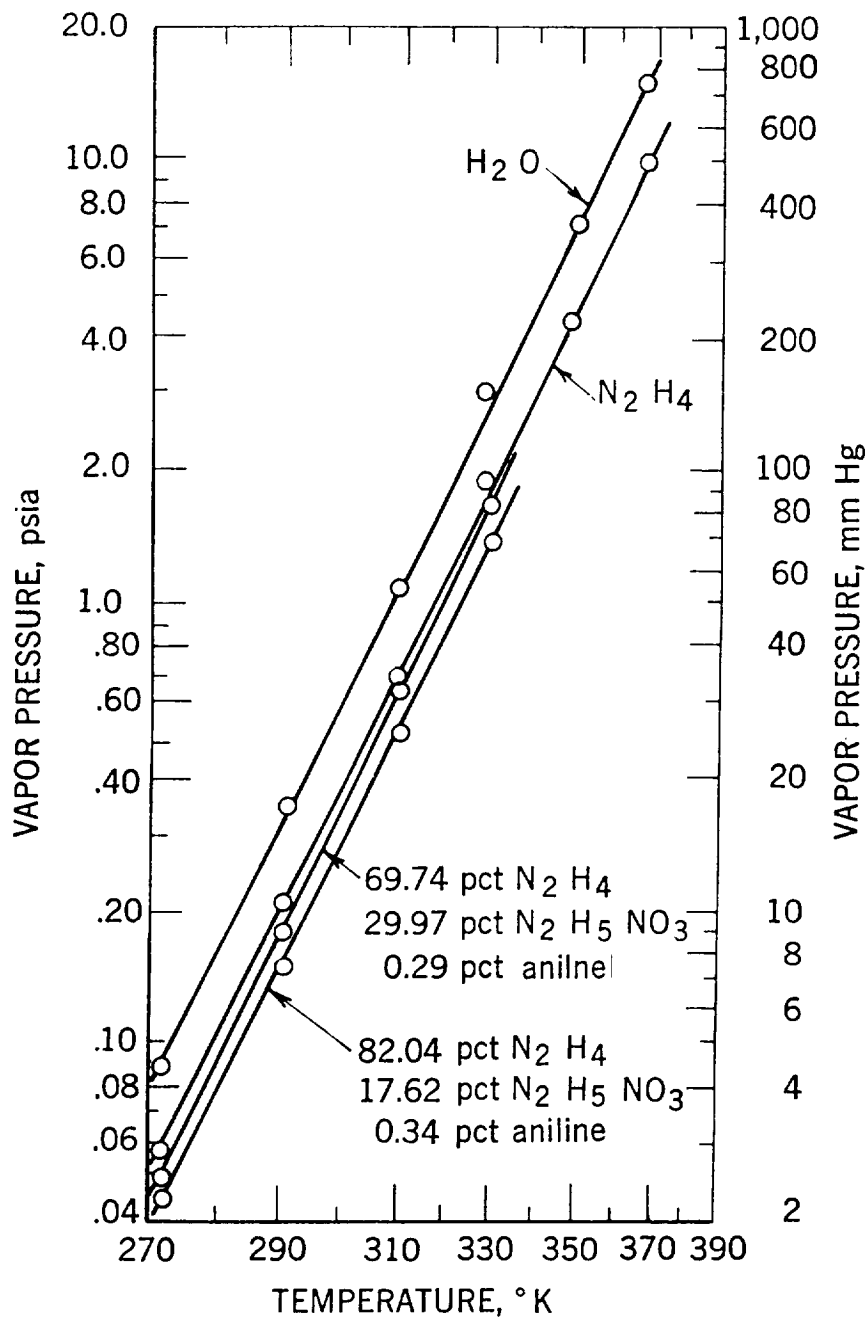Figure 19: Surface tension of molten HN, N_2H_4 and water as a function of temperature.

PX3-103
544

Figure 20: Vapor pressure of $HN-N_2H_4$ solutions and H_2O as a function of temperature.

APPENDIX II

Explosive Structural and Inertial Response of Rocket Engines

Experiments were made to determine the structural damage and the inertial response of the 100-lb thrust rocket engines to internal explosive reactions. In these experiments, 3, 6, and 7.5 grams of tetryl were fired with a No. 8 detonator at various locations in a simulated combustion chamber. The engines used in this study were machined from type 347 stainless steel and were similar in size and shape to those used in the MSC qualifying studies. Figure 21 shows the combustion chambers used in this study and the engine assembly. Six experiments were performed using various charge sizes and locations. Figure 22 shows the charge locations for three experiments using 6-gram tetryl charges. In two other experiments 3 and 7.5 grams of tetryl were fired in the mid-center position. The remaining chamber was fired with a 6-gram charge at the mid-center position in a low pressure environment. In all mid-center experiments the charge height was adjusted with a stainless steel spacer located under the detonator so that the mass center of the charge was always at the chamber center.

To conduct an experiment, the apparatus was assembled in the bombproof and the charge, consisting of one, two, or three tetryl pellets glued together with Duco cement, was cemented to the top of the detonator. The charge was fired remotely, and the final chamber volume was measured by water displacement.

The results of these experiments are shown in table 10 which gives the percent increase in the motor's maximum diameter and volume for each tetryl charge size used. The percent increase in the maximum diameter of the motor is plotted as a function of the charge weight at the center position in figure 23.

Figure 24 shows a photograph of the three engines after firing in an ambient environment using 3, 6 and 7.5 gram tetryl charges at the center location; the peen marks on the exterior surface of the motors were used to measure the eccentricity of deformation following each shot. Figure 25 shows a cutaway view of the engine fired with a 7.5-gram charge. The pitting observed near the flanged end is due to the high velocity fragments from the shell of the No. 8 detonator.

The final experiments in this series were conducted with 6-gram tetryl charges located at the low-center and side-center positions as shown in figure 22. The purpose was to investigate the effect of charge location on explosive damage. Figure 26 shows the motors after each of these shots. It can be seen that moving the charge off the axis of the motor has a pronounced effect on the resulting damage.

TABLE 10. - Changes in Motor Volume and Diameter

Charge,[1]	Charge location	Volume increase percent	Diameter increase percent
3.0	Center	4.92	2.50
6.0	Center	10.72	12.45
7.5	Center	19.15	20.10
6.0	Side-center	--[2]	--
6.0	Mid-low	9.05	12.85
6.0[3]	Center	12.70	15.00

1/ Weight of pressed tetryl pellets exclusive of No. 8 detonator.

2/ This motor exhibited a weight loss of 9.3 gm.
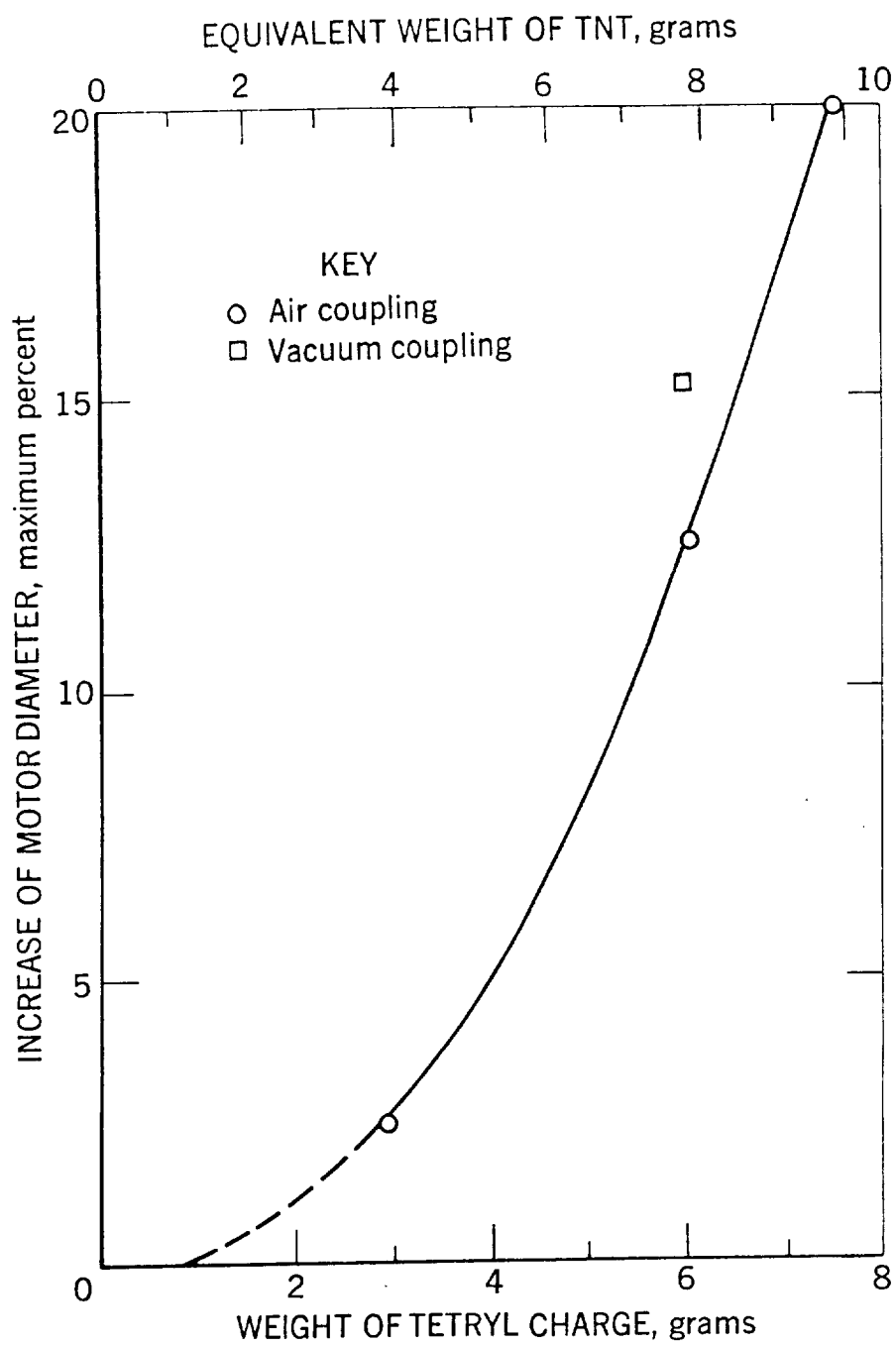
3/ Fired in environmental pressure of < 1 torr.

3 gram−tetryl
pellet

Dupont No. 8
blasting cap

Top flange

Bottom flange
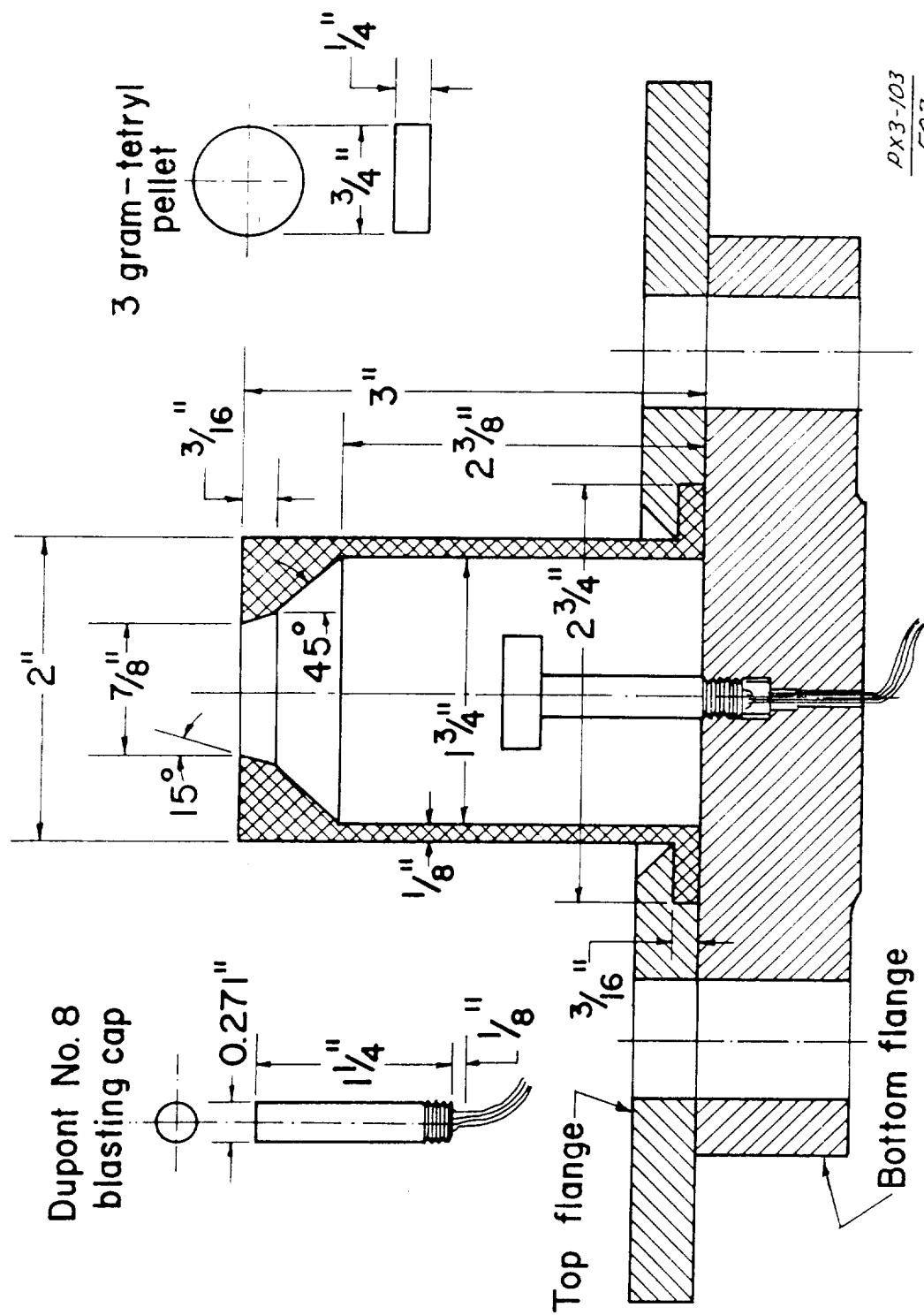
$\frac{px3-103}{507}$

Figure 21: Cross section of simulated rocket engine combustion
chamber and test assembly.
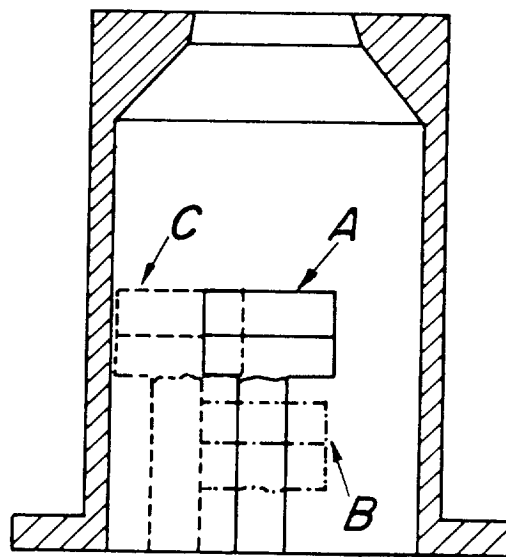
$$\frac{px3-103}{505}$$

Figure 22: Location of charges in the combustion chamber:
A - center, B - low center and C - side center.

EQUIVALENT WEIGHT OF TNT, grams

KEY
○ Air coupling
□ Vacuum coupling

INCREASE OF MOTOR DIAMETER, maximum percent

WEIGHT OF TETRYL CHARGE, grams

PX3-103
543

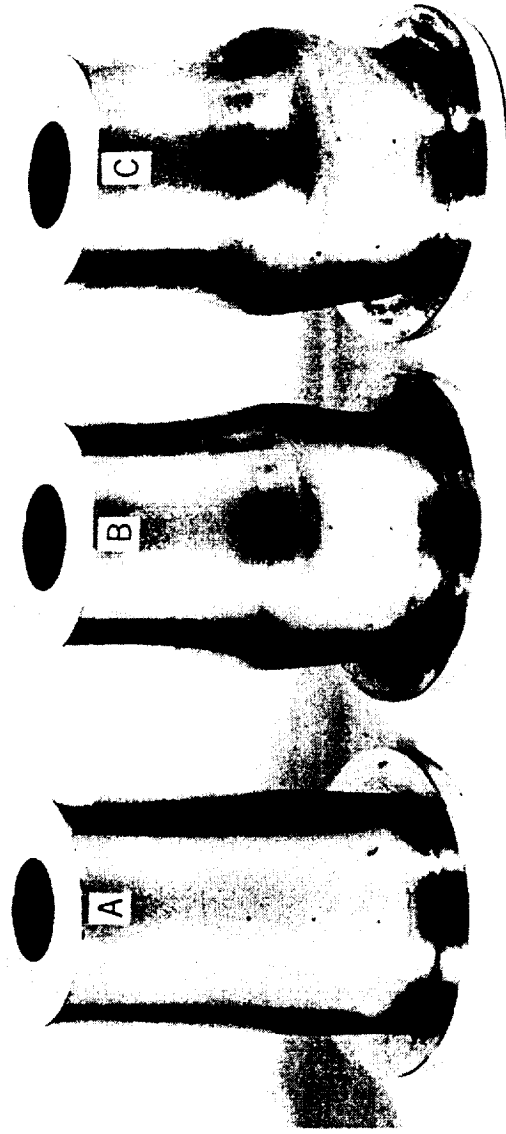Figure 23: Percent increase in motor volume as a function of the charge size.

Figure 24: Photograph of engines after firing with 3 (A), 6 (B) and 7.5 grams (C) of tetryl at the chamber center.

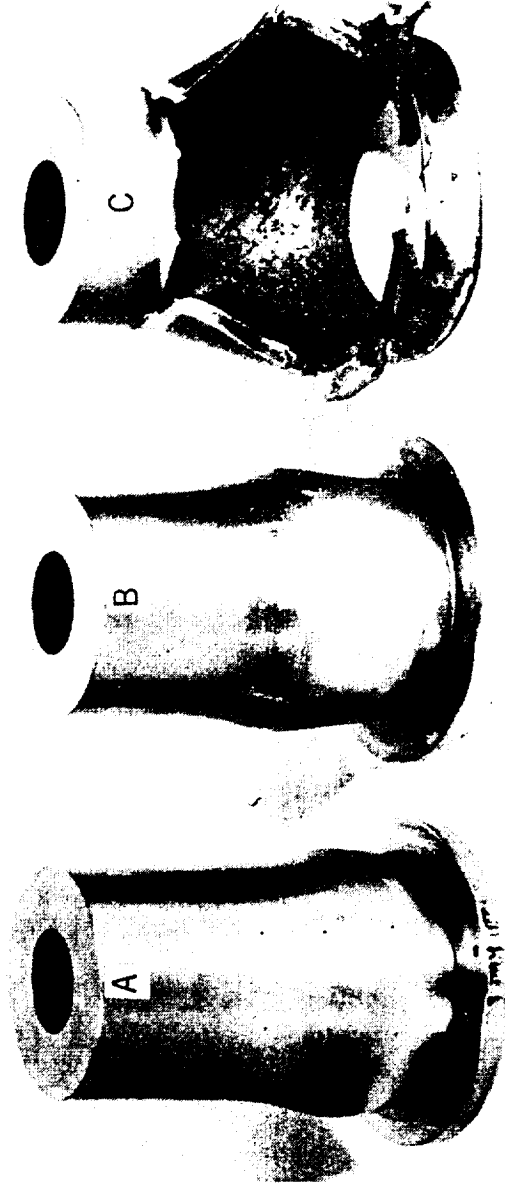Figure 25: Cross section of the engine after fired with a 7.5 gm charge at the center of the chamber.

Figure 26: Photograph of engines after firing with 6 grams tetryl at the low-center (A), center (B), and side center (C) positions.

Furthermore, in the low-center and center experiments, the resulting
motor deformation is not significantly different. The percentage change
in volume for the low-center shot is smaller than for the center shot, but
the converse is true for the corresponding change in maximum diameter,
indicating that the contour of the deformed surface in the low-center shot
is more sharply tapered than in the center one. Apparently, this is due
to the presence of the flange near the deformed area.

Since it is known that the condition of the atmosphere surrounding an
explosion can have a significant effect on the dynamics of the resulting
blast wave, an additional experiment was conducted to investigate the
effect of low combustion chamber pressures on the damage potential of the
explosion. In this experiment a 6-gram tetryl charge placed at the center
position was fired in a motor located in an evacuated bell-jar ($<$1 torr).
These results are shown in table 10. The percent volume increase in the
motor volume (12.7 percent) at low pressure compared with that at atmos-
pheric pressure (10.7 percent) is not sufficient to show an effect of the
initial chamber pressure on the deformation process. This was expected since
the shock pressure in the blast wave of the explosion is many orders of
magnitude greater than the ambient pressure, consequently, the effect of
the latter should be insignificant. From Loving's relationship and yield
strength values for type 347 stainless steel of 30×10^3 to 120×10^3 psia, it
was estimated that 0.7 to 3 grams of TNT should be capable of damaging
the simulated MSC engines. The results shown in figure 24 agree with these
findings in that a minimum of about 1 to 3 grams of TNT is required to
permanently deform these engines. This suggests that Loving's relationship
does give representative values for the limiting quantity of explosive
required to damage these engines. Ten grams of TNT appears to be the
maximum explosive charge these stainless steel engines can sustain without
rupture of their walls.

The reflected explosion shock pressures delivered to the engine walls
by these explosions were also measured. The explosive charge was fired in
a thick-walled combustion chamber, machined from cold rolled steel, having
the same internal geometry and dimensions as the previous engines. The
resistive pressure transducer used in the thin film studies was used for
recording the peak reflected pressure. Figure 27 shows the thick walled
engine, charge location, and the related circuitry for the experiment. The
scopes used to monitor the resistance output signal were triggered by means
of a twisted pair of wires located next to the detonator. Table 11 gives the
experimental peak reflected shock pressures obtained from the oscillograms
for the various shots using 3, 6, and 9 grams of tetryl and No. 8 detonator;
the confidence intervals shown in the table represent 90 percent values. The
peak reflected pressures appear to increase approximately as the square root
of the mass of the charge. Although these peak pressures are quite large
they are also short lived (of the order of microseconds) so that the resulting
impulse is considerably less than the magnitude of the pressure suggests.

TABLE 11. - Peak Reflected Shock Pressures Resulting from the Explosion of Various Weights of Tetryl

Total[1] Charge Weight (grams of TNT)	Number of trials	Peak reflected shock pressure (X 10^3 psi)
4.65	6	85 ± 20
8.58	3	100 ± 30
12.41	2	130 ± 20

1/ Combined weight of tetryl pellet and detonator, expressed in TNT equivalent weight.
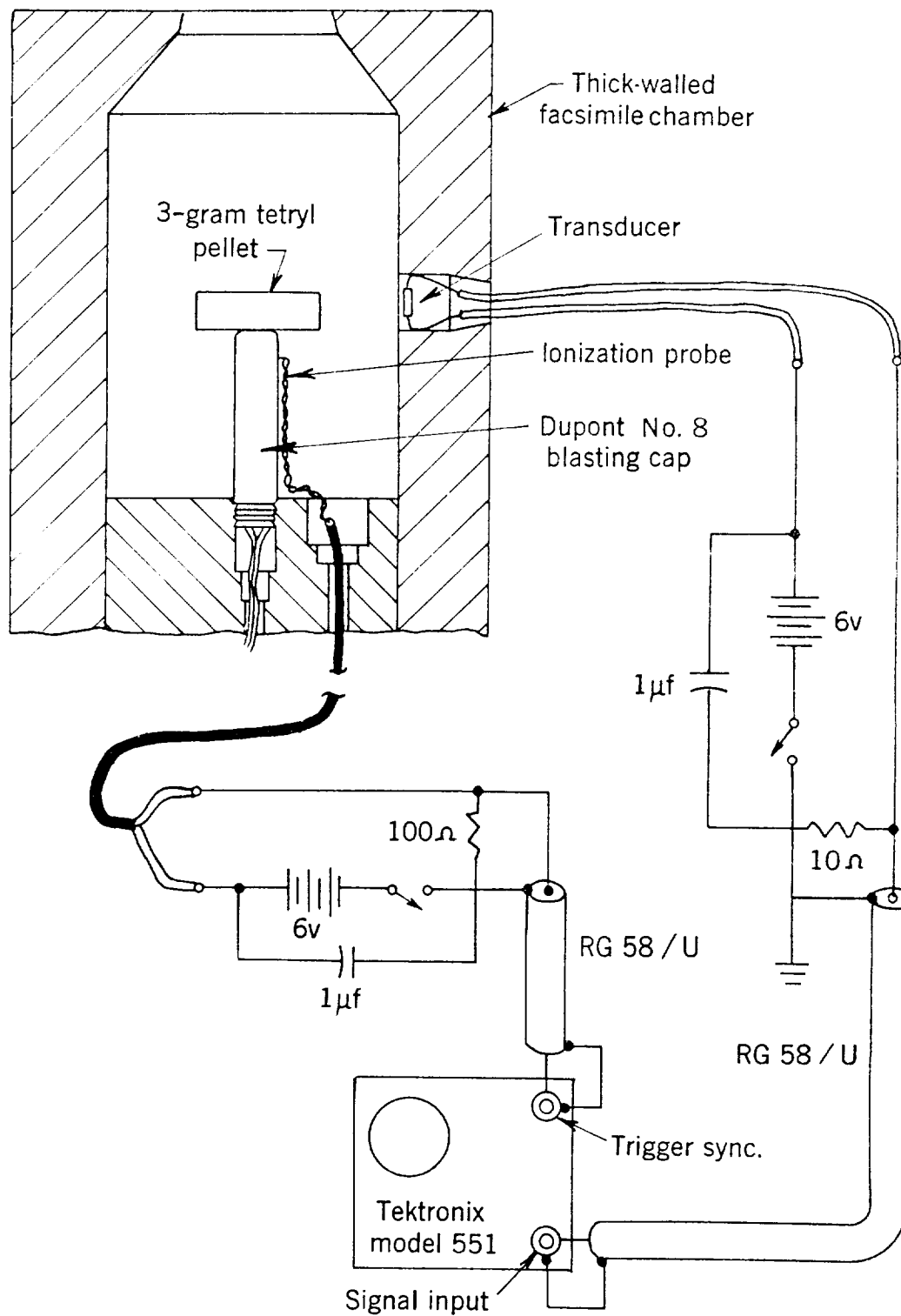
Figure 27: Apparatus used to measure the reflected shock pressure resulting from combustion chamber explosions.

The thrust imparted to these engines by an interval explosion is the result of two forces--the blast wave interaction with the interior surface of the engine, and the escape of the explosion products out the throat. An explosion in the reaction chamber of the rocket engine generates a blast wave, one part of which travels out of the throat while another part is reflected off the injector face. Since the blast wave striking the injector imparts a forward motion to the engine and the wave leaving the nozzle contributes only a negligibly small rearward thrust, the blast wave per se contributes a net measurable forward thrust to the engine. As the blast waves continue to reflect from the engine's internal surfaces and to interact, the chamber pressure approaches a uniform value. It can be shown that the time necessary for pressure equalization in these chambers is of the order of 20 microseconds. When the pressure is equalized, the hot compressed product gases escaping from the nozzle provide an added thrust. This thrust can be calculated from Rodean's rocket thrust transient equations.[42/] For an assumed gas product chamber temperature of 3,000°K, Rodean's equation shows that the chamber pressure drops 90 percent of its initial value within 500 microseconds. Therefore, pressure equalization is approximately 25 times faster than the product gas exhaust process; thus, we are justified in partitioning the engine thrust into two segments. To calculate the thrust imparted to the engine by the escaping product gases, it is necessary to know the initial pressure in the combustion chamber following pressure equalization. This pressure can be obtained from experiments using the ballistic mortar. Knowing the simple kinematic description of the ballistic mortar and the response of the mortar to the explosion of various weights of explosives, an effective explosion pressure of 5,000 psi was obtained for 9-gram charge of TNT. Using this value for the initial explosion product gas pressure and Rodean's transient thrust relationships, a total impulse of 2×10^5 dyne-sec was obtained.

The ballistic mortar was used to measure the impulse delivered to these engines from these explosive reactions in the combustion chamber. In these experiments, the thick-walled engine, previously used in the blast pressure experiments, was machined to fit snugly in the mortar, in place of the firing chamber. The projectile was not used, as the purpose was to measure the thrust imparted to the mortar by the explosion products escaping from the engine. Three, 6 and 9 grams of tetryl, respectively, were glued to the top of a No. 8 detonator and were used as the explosive charge. The engines were loaded and the experiments were conducted in much the same way as the previous experiments using the ballistic mortar. From the response of the mortar the impulsive response of the explosion was determined. Figure 28 shows the results of these experiments. An equivalent 9-gram TNT charge, for example, results in an impulse of 2×10^6 dyne-sec. This is an order of magnitude greater than the impulse calculated above for the product gas exhaust process, indicating that the reflection of the blast wave from the injector face accounts for the major portion of the impulse,
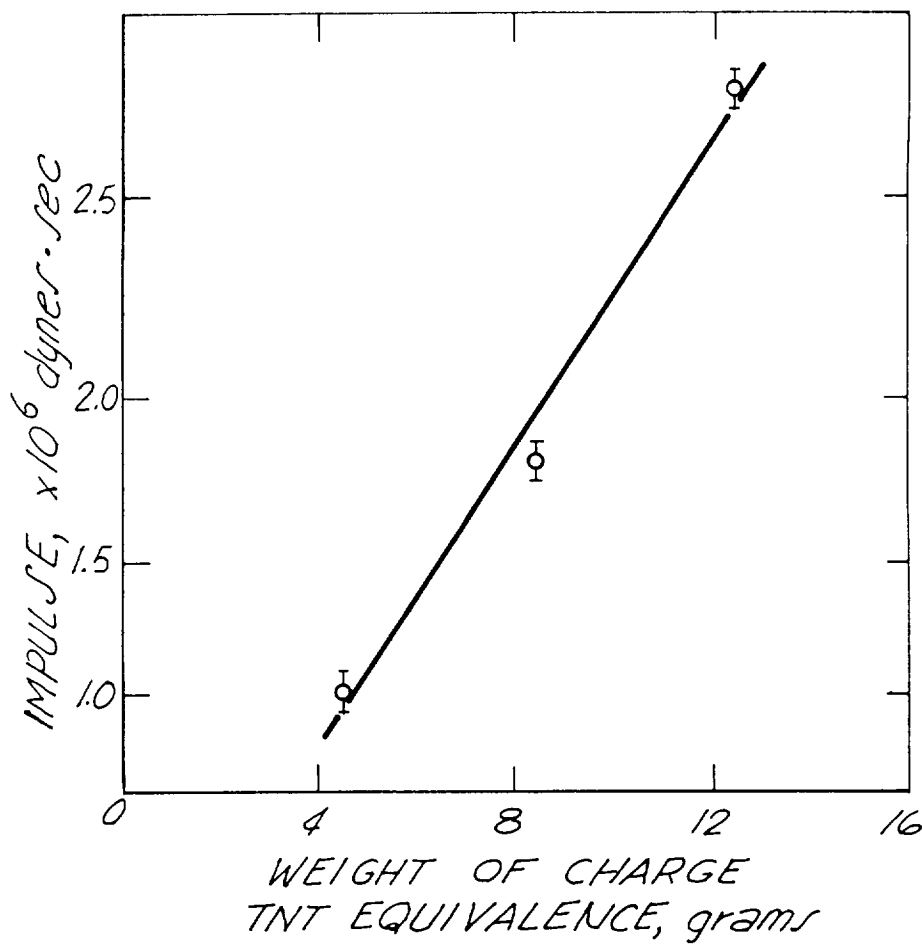
Figure 23: Rocket engine impulse resulting from internal explosions of various weights of explosive.

or about 1.8×10^6 dyne-sec. Using this value and the mean peak explosion pressure of 30×10^5 psia for the 9-gram TNT charge (table 11) and assuming that the explosion pressure pulse if triangular in shape, it can be shown that this 2×10^6 dyne-sec impulse corresponds to a half-life of about 150 microseconds for the reflected pressure pulse.

REFERENCES

1. Zeldovich, Ia. B., and A. S. Kompaneets. Theory of Detonation, Academic Press, New York, N. Y., 1960, p. 84.

2. Loving, F. A. Barricading Hazardous Reactions, Ind. Eng. Chem., v. 49, October 1957, pp. 1744-1746.

3. Scott, F. E., J. J. Burns, and B. Lewis. Explosive Properties of Hydrazine, Bureau of Mines Rept. of Inv. 4460, 1949, 18 pp.

4. Herickes, J. A., G. H. Damon and M. G. Zabetakis. Determining the Safety Characteristics of Unsymmetrical Dimethylhydrazine, Bureau of Mines Rept. of Inv. 5635, 1960, 12 pp.

5. Jost, W. Investigation of Gaseous Detonations and Shock Wave Experiments with Hydrazine, Aeronautical Research Laboratories, Office of Aerospace Research, Wright-Patterson Air Force Base, Ohio, ARL-62-330, April 1962, p. 74.

6. Heinrich, H. J. The Propagation of Detonation in Hydrazine Vapor, Zeitschrift fur Physikalische Chemie Nene Folge, v. 42, 1964, pp. 149-165.

7. Minton, S. J., and E. B. Zwick, "An Investigation of Manifold Explosions in a Rocket Engine." Paper presented at the 3rd ICRPG Combustion Conference, John F. Kennedy Space Center, NASA, Cocoa Beach, Florida, October 17-21, 1966.

8. Ivany, R. D. Collapse of a Cavitation Bubble in Viscous, Compressible Liquid-Numerical and Experimental Analysis, NASA Scientific and Technical Information Center, Rept. No. N65-33866, August 1966, p. 201.

9. Naude, C. F., and A. T. Ellis. On the Mechanism of Cavitation Damage by Nonhemispherical Cavities Collapsing in Contact with a Solid Boundary, Trans. Am. Soc. Mech. Engrs., J. Basic Eng., v. 83, 1961, p. 648.

10. Shutler, N. D., and R. B. Mesler. A Photographic Study of the Dynamics and Damage Capabilities of Bubbles Collapsing Near Solid Boundaries, Trans. Am. Soc. Mech. Engr., J. Basic Eng., v. 87, 1965, p. 511.

11. Benjamin, T. B., and A. T. Ellis. The Collapse of Cavitation Bubbles and the Pressures Thereby Produced Against Solid Boundaries.

12. Watson, R. W., and F. C. Gibson. Jet from Imploding Bubbles, Nature, v. 204, No. 4965, December 26, 1964, pp. 1296-1298.

13. Williams, F. A. Progress in Spray-Combustion Analysis, Eighth International Symposium on Combustion, The Williams and Wilkins Company, Baltimore, Md., 1962, pp. 50-69.

14. Webber, W. F. Spray Combustion in the Presence of a Traveling Wave, Eighth International Symposium on Combustion, The Williams and Wilkins Company, Baltimore, Md., 1962, pp. 1129-1140.

15. Cramer, F. B. The Onset of Detonation in a Droplet Combustion Field, Ninth International Symposium on Combustion, Academic Press, New York, N. Y., 1963, pp. 482-487.

16. Busch, C. W., A. J. Laderman, and A. K. Oppenheim. Parametric Study of the Generation of Pressure Waves by Particle-Fueled Combustion, AIAA Second Annual Meeting and Technical Demonstration, San Francisco, Calif., paper 65-357, July 1965.

17. Dabora, E. K., K. W. Ragland, and J. A. Nicholls. A Study of Heterogeneous Detonations, Astronautica Acta, v. 12, No. 1, 1966, pp. 9-16.

18. Loison, R. The Mechanism of Explosions in Compressed Air Pipe Ranges, Seventh International Conference of Directors of Safety in Mines Research, Buxton, England, 1952.

19. Gordeev, V. E., V. F. Komov, and Ya. K. Troshin. Concerning Detonation Combustion in Heterogeneous Systems, Proc. of the Academy of Sciences, U.S.S.R., v. 160, No. 4, 1965.

20. Stern, R. A., A. J. Laderman, and A. K. Oppenheim. Statistical Study of Accelerating Flames, The Physics of Fluids, v. 3, No. 1, January-February 1960, pp. 115-120.

21. Bollinger, L. E., and R. Edse. Wright Air Development Center Technical Rept. 58, 1959.

22. Weiss, H. G. A Basic Study of the Nitrogen Tetroxide-Hydrazine Reactions, Dynamic Science Corporation, SN-4500, July 1965, 50 pp.

23. Seamans, T. F., and B. E. Dawson. Hypergolic Ignition at Reduced Pressures, Air Force Rocket Propulsion Laboratory, Technical Rept. AFRPL-TR-67-129, June 1967, pp. 125.

24. Curtius, T., and R. Jay. J. Praktische Chemie, v. 39, 1889, p. 45.

25. Michel, R. E., G. G. Harms, J M. Koepche, R. W. Mueller, W. O. Jacobson, J. R. Syolund, and N. G. Christians. Detonation Reaction Control (Small Impulse Engine), Air Force Flight Dynamics Laboratory, Wright-Patterson Air Force Base, Technical Documentary Report No. FDL-TDR-64-63, March 1964, 90 pp.

26. Shidlovskii, A., V. I. Semishin, and V. I. Simutin. Thermal Decomposition and Combustion of Hydrazine Nitrate, Zhurnal Prikladnoy Khimii, v. 33, No. 6, 1960, pp. 1411-1413.

27. Moran, H. E., J. C. Burnett, and E. I. Smith, Jr. Explosion Hazards of Mixed Hydrazine Fuel, Naval Research Laboratory Memorandum Rept. 1615, May 1965, 13 pp.

28. Price, D., T. P. Liddiard, Jr., and R. D. Drosd. The Detonation Behavior of Hydrazine Nitrate, U. S. Naval Ordnance Laboratory, NOLTR-66-31, April 15, 1966, 15 pp.

29. Eyster, E. H., L. C. Smith, and S. R. Walton. The Sensitivity of High Explosives to Pure Shocks, Naval Ordnance Laboratory Memorandum 10-336, July 14, 1949, p. 39.

30. Dwiggins, R. D., and B. F. Larrick. Investigation of Mixtures of Hydrazine, Hydrazine Nitrate, and Water, Part III - Progress Report Covering the Period from April 1 to June 30, 1952, Naval Ordnance Laboratory, NAVORD Report 2563, August 13, 1952, 77 pp.

31. Furman, N. H. (ed.). Scotts Standard Methods of Chemical Analysis, 5th Edition, D. Van Nostrand, 1939, p. 635.

32. Perlee, H. E., A. C. Imhoff, and M. G. Zabetakis. Flammability Characteristics of Hydrazine-Unsymmetrical Dimethylhydrazine-Nitrogen Tetroxide-Air Mixtures, Explosives Research Laboratory Final Rept. No. 3806, February 15, 1961, 17 pp.

33. Willoughby, A. B., J. Mansfield, T. C. Goodale, and C. Wilson. Summary of Existing Information Concerning the Explosive Potential of the Hypergolic Propellant Combination N_2O_4/50% N_2H_4, AFRPL-TR-6527, April 1965, 109 pp.

34. Gibson, F. C., M. L. Bowser, C. R. Summers, and F. H. Scott. An Electrical Method for the Continuous Measurement of Propagation Velocities in Explosives and Propellants, Bureau of Mines Rept. of Inv. 6207, 1963, 8 pp.

35. Watson, R. A Gauge for Determining Shock Pressures, Review of Scientific Instruments, v. 38, No. 7, July 1967, pp. 978-80.

36. Robinson, R. J., and W. C. McCrone. Hydrazine Nitrate (1) Analytical Chemistry, v. 30, 1958, pp. 1014-1015.

37. Medard, L. Explosive Properties of Hydrazine Nitrate, Memorial des Poudres, v. 34, 1952, pp. 147-157.

38. Kissinger, L. W. The Penetration and Properties of Hydrazine Nitrate, Naval Ordnance Laboratory Memorandum 10,359, July 7, 1949, p. 4.

39. Corcoran, J. M., W. H. Kruse, S. Skolnik, and F. Lieber. Thermal Analysis of the System Hydrazine Nitrate - Water - Hydrazine, U. S. Naval Ordnance Test Station, NAVORD Rept. 2087, January 1954, 13 pp.

40. Vango, S. P., and J. B. Krasinsky. Density, Vapor Pressure and Viscosity of Solutions of Hydrazine Mononitrate in Hydrazine. Jet Propulsion Laboratory, Technical Memorandum No. 33-103, October 15, 1962, 12 pp.

41. Partington, J. R. An Advanced Treatise of Physical Chemistry,
     v. 2, The Properties of Liquids, Tungmans, Green and Company,
     1951, p. 185.

42. Rodean, H. C. Rocket Thrust Termination Transients, ARS Journal,
     June 1959, pp. 406-409.

41. Partington, J. R. An Advanced Treatise of Physical Chemistry,
     v. 2, The Properties of Liquids, Tungmans, Green and Company,
     1951, p. 185.

42. Rodean, H. C. Rocket Thrust Termination Transients, ARS Journal,
     June 1959, pp. 406-409.

DISTRIBUTION LIST

Reproducible and 3

Carl Hohmann - EP 421
NASA Manned Spacecraft Center
2101 Webster-Seabrook Road
Houston, Texas 77058

1

R. J. Rollbuhler
Mail Stop 21-5
NASA, Lewis Research Center
Cleveland, Ohio 44101

1

Robert F. Rose
Chief, Propulsion Division
NASA, Jet Propulsion Laboratory
4800 Oak Park Drive
Pasadena, California 91102

1

Jerry Thompson
Propulsion and Vehicle Engineering
NASA, Marshall Space Flight Center
Hunstville, Alabama 35801

1

David Winterhaulter
Office of Manned Space Flight - Code MAT
NASA Headquarters
Washington, D. C. 20013

1

Robert Rollins
NASA Headquarters - Code RPT
Washington, D. C. 20013

1

Major W. S. Moe
Chief, Liquid Rocket Division
Air Force Rocket Propulsion Laboratory (RPR)
Edwards, California 93523

3

NASA Manned Spacecraft Center
Technical Information Division/BF33
2101 Webster-Seabrook Road
Houston, Texas 77058
Attention: Retha Shirkey

1

NASA Manned Spacecraft Center
General Research Procurement Branch/BG751
2101 Webster-Seabrook Road
Houston, Texas 77058
Attention: Robert N. Bailey

U.S. Gov't

Recipient	Copies

Ervin Johnson
Lewis Research Center
21000 Brook Park Road
Cleveland, Ohio 44101

1

Chemical Propulsion Information Agency
The John Hopkins Applied Physics Laboratory
8621 Georgia Avenue
Silver Spring, Maryland 20910
Attention: Thomas Christian

1

U.S. Gov't